CHARACTERIZATION OF THE OPTICAL PROPERTIES OF SEAWATER FROM THE DEEPWATER HORIZON OIL SPILL

A Thesis

by

ANTHONY MARKUS TODD

Submitted to the Office of Graduate and Professional Studies of
Texas A&M University
in partial fulfillment of the requirements for the degree of

MASTER OF MARINE RESOURCES MANAGEMENT

Chair of Committee,	Rainer M.W. Amon
Committee Members,	Karl Kaiser
	Norman L. Guinasso Jr.
Head of Department,	Kyeong Park

May 2016

Major Subject: Marine Resources Management

ABSTRACT

The fluorescence and absorbance optical properties of seawater samples from the Deepwater Horizon (DWH) oil spill were analyzed to examine the transport and fate of oil both during and after the spill, as well as the effect of chemical dispersant on the optical properties. Seawater samples were collected during three cruises: in June 2010, when the well was still discharging oil, in September 2010, after the well had been capped, and in January 2016 in an area around the Taylor Energy site, which has been leaking oil since Hurricane Katrina. Two excitation/emission wavelength pairs were chosen to trace oil from the DWH spill based on fluorescence excitation/emission matrices (EEMs) of seawater samples: 275/324 nm and 240/354 nm. These pairs were chosen based on similarities to oil signatures from the literature, as well as in situ sensor responses at corresponding depths showing decreases in dissolved oxygen, increases in CDOM, decreased transmission and increased chlorophyll for June samples, and decreases in dissolved oxygen, increased CDOM, depletions in the $\delta^{13}C$ of DIC, and enrichments in DIC for September samples. Increases in fluorescence intensity values at these chosen wavelength pairs provided evidence of crude oil from the Macondo well between 900 m and 1200 m depth at several stations in June, and between 1000 m and 1200 m depth at several stations in September. Fluorescence EEMs from the Acadiana station with known fresh surface oil were compared to EEMs from June and September stations to identify the presence of oil, although massive inputs from Mississippi River floodwaters complicated interpretation. Fluorescence intensity values of the 275/324 nm

and 240/354 nm wavelength pairs at the surface and around 1100 m depth were used to generate maps showing the spatial distribution of oil from June to September. Samples exhibiting signatures similar to oil were generally found at a distance of up to 10 miles both southwest and northeast of the well in June and extended to the southwest almost 300 miles from the well in the months following the spill.

ACKNOWLEDGEMENTS

I would like to thank my committee chair, Dr. Amon, and my committee members, Dr. Kaiser and Dr. Guinasso, for their guidance throughout the course of this research. I am truly thankful for their support and for the opportunity to participate in this research. I would also like to thank my mother and father for their encouragement and support throughout my academic career.

TABLE OF CONTENTS

Page

1. INTRODUCTION…….. 1

2. METHODS……...11

2.1 Measurement of fluorescence EEMs……..14
2.2 Measurement of UV-absorption and spectral slope……15
2.3 Measurement of in situ data……17

3. RESULTS……19

3.1 June samples……... 19
3.1.1 Proxy in situ data…… 19
3.1.2 Spectral slope and slope ratio…….. 22
3.1.3 Fluorescence intensity ratio……23
3.2 September samples…… 25
3.2.1 Proxy in situ data…… 25
3.2.2 Spectral slope and slope ratio……..…… 29
3.2.3 Fluorescence intensity ratio……...……... 30
3.3 Acadiana cruise samples……31
3.3.1 Proxy in situ data…… 31
3.3.2 Spectral slope and slope ratio……..…… 34
3.3.3 Fluorescence intensity ratio……35

4. DISCUSSION……...37

4.1 Excitation/emission wavelength pairs representative of oil……... 37
4.1.1 275/324 nm…….. 37
4.1.2 240/354 nm…….. 39
4.1.3 Comparison to background signal……... 41
4.2 Characterization of June samples……...…… 44
4.3 Characterization of September samples……..46
4.4 Characterization of Acadiana cruise samples……48
4.5 Spatial distribution of optical oil indicators……50

5. CONCLUSIONS…….. 55

REFERENCES…… 57

LIST OF FIGURES

Page

Figure 1 Map of station locations in the northern Gulf of Mexico for all stations and June stations……..12

Figure 2 Map of station locations in the northern Gulf of Mexico for September stations and the Acadiana cruise station……..…….……13

Figure 3 Plot of temperature, salinity, and potential density anomaly vs. depth, and salinity vs. temperature from station 4 (June 2010)…….....20

Figure 4 Plot of oxygen, CDOM, transmission, and chlorophyll in situ data from station 4 (June 2010)……21

Figure 5 Plot of $S_{275\text{-}295}$ and S_R values for June stations as a function of depth…….. 23

Figure 6 Plot of FIR values for June stations as a function of depth……...24

Figure 7 Plot of temperature, salinity, and potential density anomaly vs. depth, and salinity vs. temperature from station 20 (September 2010)……... 26

Figure 8 Plot of oxygen, CDOM, $\delta^{13}C$ of DIC, and DIC in situ data from station 20 (September 2010)…… 27

Figure 9 Relationship between oxygen values and the $\delta^{13}C$ of DIC, and CDOM and $S_{275\text{-}295}$……..…….. 29

Figure 10 Plot of $S_{275\text{-}295}$ and S_R values for September stations as a function of depth……...……... 30

Figure 11 Plot of FIR values for September stations as a function of depth…..... 31

Figure 12 Plot of temperature, salinity, and density vs. depth, and salinity vs. temperature from the Acadiana station……..32

Figure 13 Plot of oxygen and CDOM in situ data from the Acadiana station…….....33

Figure 14 Plot of $S_{275\text{-}295}$ and S_R values for the Acadiana station as a function of depth…… 35

Figure 15 Plot of FIR values for the Acadiana station as a function of depth.....36

Figure 16 Fluorescence intensity plotted vs. depth for the 275/324 nm and 260/450 nm signals……..... 39

Figure 17 Fluorescence intensity plotted vs. depth for the 240/354 nm and 270/308 nm signals…….…... 40

Figure 18 EEMs of background deep water marine dissolved organic matter from station 22 at 2000 m depth (September 2010), background surface marine dissolved organic matter from station 22 at 50 m depth (September 2010), the 275/324 nm peak from station 19 at 1078 m depth (September 2010), the 240/354 nm peak from station 4 at 1089 m depth (June 2010), the sample at 2 m depth (Acadiana), and the sample at 112 m depth (Acadiana)….....43

Figure 19 Spatial maps for June samples showing fluorescence intensity values at the surface for 275/324 nm and 240/354 nm, and between 900m and 1200 m depth for 275/324 nm and 240/354 nm…….……....52

Figure 20 Spatial maps for September samples showing fluorescence intensity values at the surface for 275/324 nm and 240/354 nm, and between 900m and 1200 depth m for 275/324 nm and 240/354 nm…….……...54

LIST OF TABLES

Page

Table 1 Seawater dissolved organic matter signatures……..……...4

Table 2 Fluorescence signatures of crude oil from seawater samples and extracted samples…….…… 5

Table 3 Fluorescence signatures of dispersed oil and dispersant components……. 6

Table 4 Fluorescence signatures of degraded oil…….……..8

1. INTRODUCTION

The explosion of the Deepwater Horizon (DWH) oilrig in April 2010 in the northern Gulf of Mexico discharged over 800 million liters of oil at ~1500 m depth into the surrounding water column (Zhou & Guo, 2012), and is regarded as the largest accidental oil spill in U.S. waters (Li, 2014). Due to the magnitude of the spill, responders utilized a number of different approaches to minimize potential damage to the environment, including the use of Corexit chemical dispersant. Over 6.5 million liters of dispersant were discharged at the surface and into the water column (Mendoza et al., 2013). When applied to oil, chemical dispersants decrease the tension at the oil-water interface, which breaks the oil up into smaller droplets, causing neutrally buoyant droplets to remain suspended and dissipated in a subsurface plume (Conmy et al., 2014). Previous studies have observed the subsurface plume associated with the DWH spill at depths of 1100 m to 1200 m at various locations around the Macondo wellhead (Mendoza et al., 2013; Zhou et al., 2013a). While the DWH spill has the potential to detrimentally impact the ecosystems of the marine and coastal environments (Liu et al., 2014), it also provides the opportunity to examine the transportation and fate of oil in seawater, as well as the role of chemical dispersant on the properties of oil by analyzing optical properties such as fluorescence and absorbance.

Both fluorescence and absorbance spectroscopy provide information on the composition and source of dissolved organic matter in seawater (Coble et al., 2014).

Fluorescence is a form of radiative decay in which an electronically excited molecule is relaxed through the emission of light (Lakowicz, 2006). Absorbance is a measure of the absorption properties of a fluorophore, calculated as the ratio of incident light to transmitted light (Coble et al., 2014). In order for absorption to occur, the energy of the incident light must equal the energy difference between the ground state and the excited state of the molecule (Coble et al., 2014). Both fluorescence and absorbance measurements are used to generate excitation emission matrices of oil and seawater samples.

A fluorescence excitation emission matrix (EEM) is a two-dimensional matrix of fluorescence intensity that is represented as a function of excitation on one axis and emission on the other axis (Coble et al., 2014), and can yield information on the fluorophores and functional groups in a sample (Stedmon et al., 2003). EEMs have been used to identify terrestrial, marine, and anthropogenic components of dissolved organic matter (DOM) (Stedmon & Bro, 2008), as different organic compounds fluoresce at different excitation and emission wavelengths (Bugden et al., 2008). While fluorescence spectroscopy has been shown to be a rapid and sensitive way to identify the presence of oil components (Bugden et al., 2008), the process is complicated by fluorescence signature differences due to variations in concentration, physical and chemical dispersion, and the diagenetic state of the oil (Conmy et al., 2014; Mendoza et al., 2013). It is important to note however, that a change in concentration only changes the fluorescence intensity, and not the location of excitation and emission peaks (Stedmon &

Bro, 2008). Further complicating interpretation is interference from fluorophores with similar fluorescence properties, as the fluorescence characteristics of two systems may resemble each other, but represent completely different mixtures of DOM (Jaffé et al., 2014). In particular, signals from dispersed oil can be subject to interference from humic components in coastal environments (Mendoza et al., 2013).

Dissolved organic matter in marine waters is a large reservoir of organic matter, with a definition derived from the procedure to separate a water sample into particulate and dissolved fractions by passing the sample through a submicrometer filter (Nelson & Siegel, 2002). Chromophoric dissolved organic matter (CDOM) is the portion of DOM that absorbs primarily ultraviolet and blue light (Zhou et al., 2013a). Waters that contain large amounts of CDOM have a yellowish colour, and have also been called “gelbstoff”, “yellow substance”, and “givlin” (Nelson & Siegel, 2002). In general, the structural makeup of DOM in a sample affects the location of excitation and emission peaks (Stedmon & Bro, 2008). Seawater DOM fluorescence signatures (Table 1) can be differentiated into two types: humic-like, which are found at emissions of 420-450 nm from excitations at 230-260 nm and 320-350 nm, and protein-like, which fluoresce at Ex/Em of 230, 275/300-305 nm for tyrosine-like proteins, and at 230, 275/340-350 nm for tryptophan-like proteins (Coble, 1996). Table 1 shows known fluorophores in natural waters, the wavelengths they are found at, and their source in the environment (Coble et al., 2014). Some fluorophores may show double peaks, and are represented by A_B, A_T, A_M, and A_C peak names corresponding to the main peaks they are associated with. These

characteristics allow the use of optical methods like fluorescence spectroscopy to distinguish different DOM components in water samples.

Component	Ex/Em (nm)	Peak Name	Source
Tyrosine-like	230/305 275/305	A_B B	Autochthonous
Tryptophan-like	230/340 275/340	A_T T	Autochthonous
Humic-like M	240/350-400 290-310/370-420	A_M M	Autochthonous, microbial
Humic-like C	260/400-460 320-365/420-470	A_C C	Humic, terrestrial, allochthonous

Table 1: Seawater dissolved organic matter signatures (Coble et al., 2014)

There are numerous studies that have characterized the fluorescence signatures of crude, dispersed, and degraded oil (Table 2). Polycyclic aromatic hydrocarbons (PAHs) are the portions of crude oil that influence fluorescence properties (Zhou et al., 2013a), and the presence of these components in the water column facilitates the use of fluorescence spectroscopy to examine the transportation and fate of oil. Bianchi et al. (2014) found a component related to released crude oil at an Ex/Em of 225/338 nm, while Zhou et al. (2013a) described two components related to crude oil: the dominant crude oil component located at an Ex/Em of 226/340 nm, and another crude oil component at (260-280)/311 nm. Mendoza et al. (2013) found an oil mixture at 220/380 nm, along with a component that resembled benzene/arene at 255/330 nm and another that resembled naphthalene at 270/340 nm. Zhou & Guo (2012) analyzed crude oil and

found a primary fluorescence peak at an Ex/Em of 224/328 nm, and a secondary peak at 264/324 nm, while Zhou et al. (2013b) identified three major oil components: one at 226/328 nm, another at 262/315 nm, and a third at 244/366 nm. Guinasso et al. (2012) analyzed the optical properties of dichloromethane extracts to compare samples collected in the Gulf of Mexico to the EEM spectrum of the DWH oil standard obtained from the National Institute of Standards & Technology. They report a peak in the DWH standard at 260/375 nm, as well as a peak at 230/348 nm in a sample collected from a surface oil slick. These crude oil fluorescence signatures can be compared to fluorescence EEMs produced in this study to aid in the characterization of oil from the Deepwater Horizon spill.

Signature	Ex/Em (nm)	Source
Released Crude Oil	225/338	Bianchi et al. (2014)
Dominant Crude Oil Component	226/340	Zhou et al. (2013a)
Crude Oil Component	(260-280)/311	Zhou et al. (2013a)
Oil Mixture	220/380	Mendoza et al. (2013)
Benzene/Arene Component	255/330	Mendoza et al. (2013)
Naphthalene Component	270/340	Mendoza et al. (2013)
Crude Oil Primary Peak	224/328	Zhou & Guo (2012)
Crude Oil Secondary Peak	264/324	Zhou & Guo (2012)
Oil Component	226/328	Zhou et al. (2013b)

Table 2: Fluorescence signatures of crude oil from seawater samples and extracted samples

Signature	Ex/Em (nm)	Source
Oil Component	262/315	Zhou et al. (2013b)
Oil Component	244/366	Zhou et al. (2013b)
DWH Oil Standard	260/375	Guinasso et al. (2012)
Dichloromethane Extract from surface sample	230/348	Guinasso et al. (2012)

Table 2: Continued

The application of dispersants to oil changes the fluorescence characteristics of the oil itself. Physically dispersed crude oils have excitation peaks between 240 nm and 300 nm, and emission peaks at ~350 nm and ~450 nm for low molecular weight (LMW) PAHs and high molecular weight (HMW) PAHs, respectively (Conmy et al. 2014). Similarly, Bugden et al. (2008) noted that when Corexit was added to oil, the fluorescence intensity increased in the 340 nm and 445 nm emission wavelengths. Zhou et al. (2013a) observed an intensity peak in a dispersant component at an Ex/Em of 234/376 nm with another peak at (260-290)/370 nm, while chemically dispersed oil showed an intensity peak at an Ex/Em of 260/430 nm (Table 3).

Signature	Ex/Em (nm)	Source
Physically dispersed LMW Crude Oil	240-300/350	Conmy et al. (2014)
Physically Dispersed HMW Crude Oil	240-300/450	Conmy et al. (2014)
Chemically Dispersed MC252 Crude Oil	270/325 and 260/450	Conmy et al. (2014)

Table 3: Fluorescence signatures of dispersed oil and dispersant components

Signature	Ex/Em (nm)	Source
Corexit Containing Component	235, 310/304, 415	Mendoza et al. (2013)
Dispersant Component Primary Peak	234/376	Zhou et al. (2013a)
Dispersant Component Secondary Peak	(260-290)/370	Zhou et al. (2013a)
Chemically Dispersed Oil	260/430	Zhou et al. (2013a)

Table 3: Continued

Oil degradation can occur due to photochemical or microbial degradation, displaying different fluorescence peaks than those of fresh crude oil. In the northern Gulf of Mexico, higher water temperatures and higher solar irradiance at the surface can lead to elevated levels of photochemical degradation, while microbial degradation can occur at both the surface and in the deep ocean (Liu et al., 2014). Conmy et al. (2014) noted that Macondo crude oil is lighter and contains a higher proportion of low molecular weight hydrocarbons than other crude oils, and is more readily degraded. Zhou et al. (2013a) found a component related to weathered oil at 240/355 nm, while Bianchi et al. (2014) found a weathered oil-derived signature at an Ex/Em of 220, 255/290 nm. Zhou & Guo (2012) identified a photochemically degraded signature at 264/324 nm, as well as a signature resembling microbial and photochemical degradation at 232/346 nm (Table 4).

Signature	Ex/Em	Source
Weathered Oil	240/355	Zhou et al. (2013a)
Weathered Oil	220, 255/290	Bianchi et al. (2014)
Photochemically Degraded Oil	264/324	Zhou & Guo (2012)
Microbial and Photochemically Degraded Oil	232/346	Zhou & Guo (2012)

Table 4: Fluorescence signatures of degraded oil

Measurements of dissolved oxygen, dissolved inorganic carbon, carbon isotopes and other in situ data can be used along with the optical properties of oil and seawater samples to aid in the characterization of oil components in the water column. Dissolved oxygen reaches a maximum in the photic zone caused by photosynthesis before rapidly decreasing to the minimum layer at ~400 m in the Gulf of Mexico, which is due to the oxidation of algal material (Millero, 2013). Below this minimum layer, oxygen concentrations generally increase with depth due to the advection of colder waters with higher levels of O_2 (Emerson & Hedges, 2008). Differences from these background dissolved oxygen levels at depth can be used as a proxy for the relative hydrocarbon biodegradation and oxygen drawdown rates within the plume (Camilli et al., 2010). Diercks et al. (2010) found that reduced dissolved oxygen values coupled with higher

CDOM fluorescence at depth near the DWH spill site corresponded to degradation by microorganisms. Other studies have also found that oxygen depletion was indicative of the microbial degradation of hydrocarbons (Hazen et al., 2010).

Dissolved inorganic carbon (DIC) is the total concentration of inorganic carbon dissolved in seawater, and is independent of temperature and pressure (Emerson & Hedges, 2008). Photodegradation in surface waters yields LMW CDOM and inorganic products, mainly CO and CO_2. This DIC formation strongly impacts carbon cycling, and may be related to oxygen consumption at the surface. However, it is not certain whether this DIC formation is due to oxygen-independent pathways or from reaction with molecular oxygen (Hansell & Carson, 2014). In deeper waters, the addition of CO_2 into the water column produces a shift in DIC; the CO_2 generated by aerobic oxidation processes can deplete the $\delta^{13}C$ of DIC due to depletion of ^{13}C (Aharon et al., 1992). Several studies have found that stable carbon isotopes such as the $\delta^{13}C$ of DIC can provide information on the origin and make up of hydrocarbons (Yeh & Epstein, 1981). Aharon et al. (1992) reported carbon sources depleted in the ^{13}C isotope that may indicate hydrocarbon seepage from seep sites in the northern Gulf of Mexico. They note that a maximum in the DIC profile corresponding to a decrease in the $\delta^{13}C$ of DIC was associated with samples taken above hydrocarbon seeps. Similar depletions found in the water column could be indicative of the presence of hydrocarbons from the DWH spill.

As the locations of intensity peaks in EEMs differ depending on the state of oil, fluorescence spectroscopy can be a useful technique to characterize and fingerprint oil signatures. This study attempts to characterize the fluorescence and other optical properties of oil and seawater samples from stations located near the Deepwater Horizon spill site during and shortly after the spill as well as along a southwestward track several months after the spill was stopped. Coupled with measurements of dissolved oxygen, WetLabs ECO-CDOM fluorometer (370/460 nm), and other in-situ and proxy data, we investigate how helpful optical properties are to understand the transport and fate of crude oil both with and without dispersants in the water column of the Gulf of Mexico.

2. METHODS

Sampling stations were located around the Deepwater Horizon oilrig in the northern Gulf of Mexico (Figure 1a). The first cruise occurred in June 2010, covered 21 stations, and collected a total of sixty samples (Figure 1b). Stations 7, 9, 10, and 11 were located within 2 miles of the well, while the rest of the stations were located at an average distance of 9.73 miles from the well. The second cruise occurred in September 2010, covered 19 stations and collected a total of ninety-two samples (Figure 2a). Stations 15, 17, and 18 were located less than 7 miles from the well. The remaining stations followed a southwest pattern, with the farthest station (station 22) located 343 miles from the well. Additional samples were collected on the Acadiana Cruise from January 10-13, 2016 at a station near the Taylor Energy Oil Well (Figure 2b); samples at 2 m, 15 m, 60 m, and 112 m depth were collected in an area where oil was observed on the surface. Analyzing the optical properties of these samples with known oil can aid in the characterization of samples collected during the June and September cruises.

Discrete water samples were collected from Niskin bottles mounted on a CTD rosette. Water samples were filtered immediately after collection using precombusted 0.7 μm Glass fiber filters (Whatman) and stored in the freezer until analysis. All maps and plots were generated using Ocean Data View (ODV) software (Schlitzer, 2014).

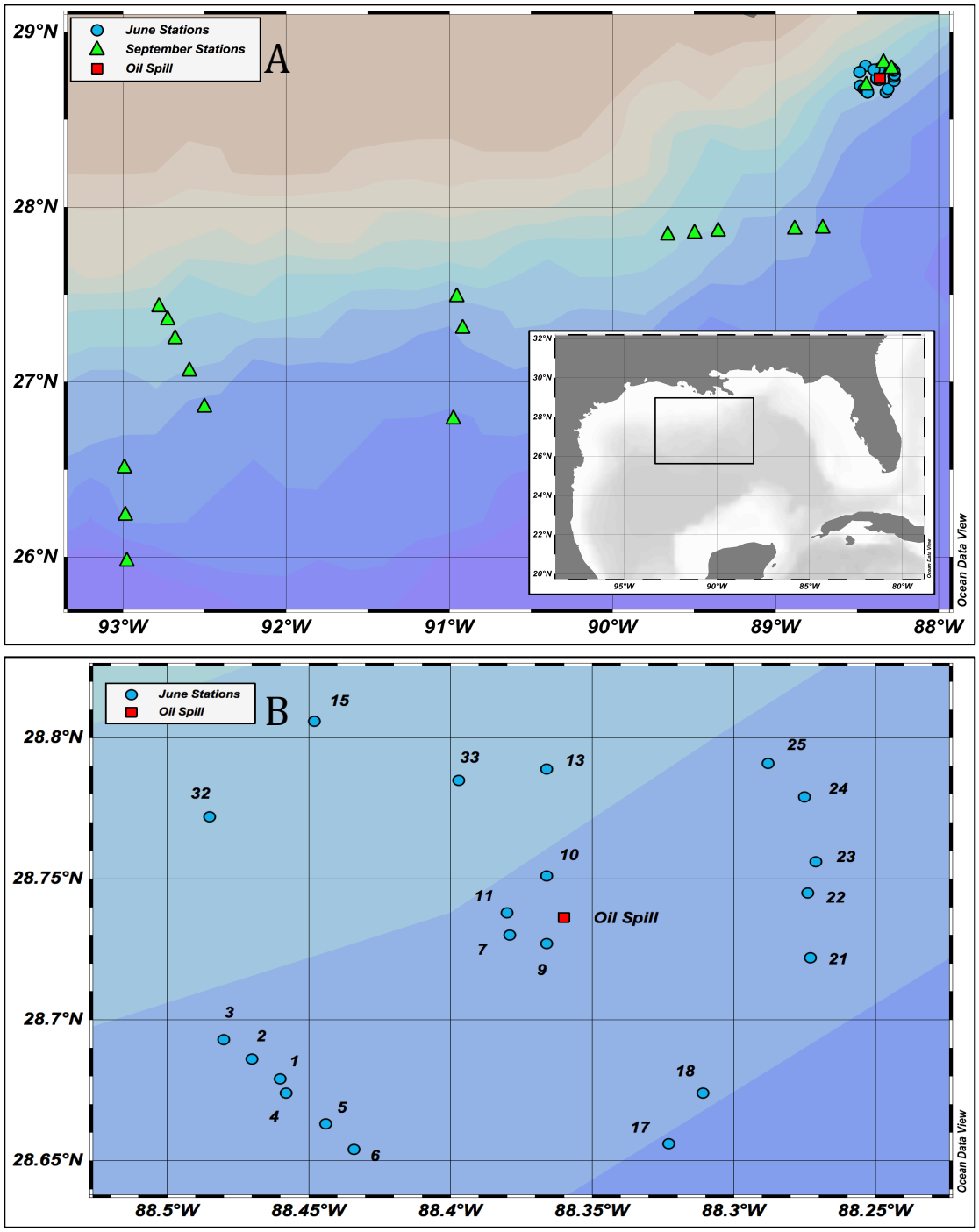

Figure 1: Map of station locations in the northern Gulf of Mexico for a) all stations and b) June stations

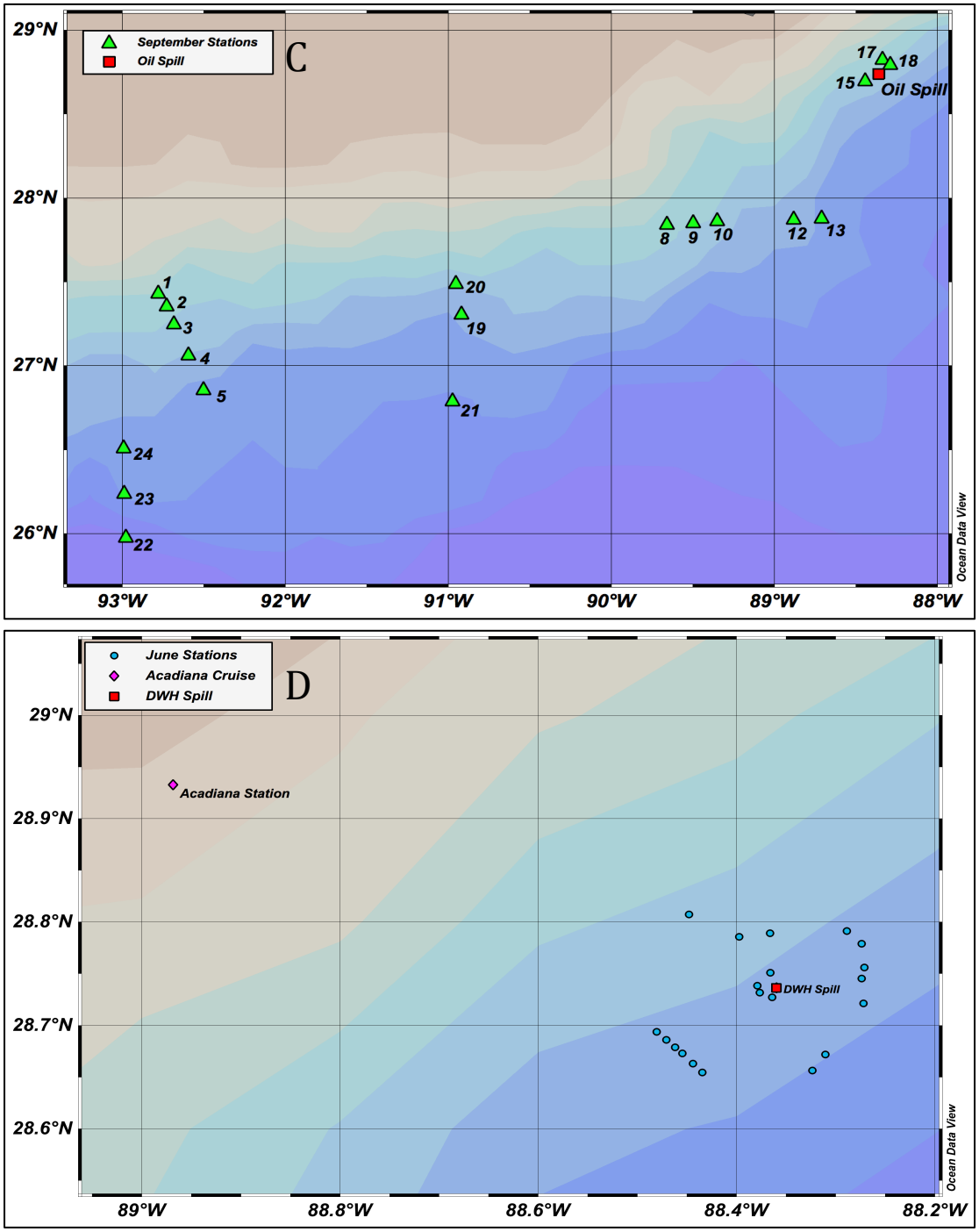

Figure 2: Map of station locations in the northern Gulf of Mexico for a) September stations and b) The Acadiana Cruise station

2.1 Measurement of fluorescence EEMs

Fluorescence spectra were collected using a Quanta Master-4 SE spectrofluorometer (Photon Technologies International) with a 1 cm cuvette and excitation and emission slit widths set to 5 nm. One hundred and fifty-one separate fluorescence emission spectra were collected from 230 to 600 nm with 2 nm intervals under excitation wavelengths from 220 to 450 nm with 5 nm intervals to obtain excitation emission matrices for each sample. Due to declining signal-to-noise ratios below excitation wavelengths of 240 nm and emission wavelengths of 300 nm, data below these wavelengths were removed (Stedmon et al., 2003). For the Acadiana Cruise samples, excitation wavelengths were collected from 220 nm to 430 nm with 2 nm intervals, and emission wavelengths were collected from 280 nm to 600 nm with 5 nm intervals to obtain excitation emission matrices for each sample.

Rayleigh and Raman scattering can cause distortions in the fluorescence signal of a sample, and so need to be corrected. The first order Rayleigh scatter line is located at wavelengths where emission equals excitation, while the second order Rayleigh scatter line is located where emission equals twice the excitation. The Raman scatter line is located at a certain energy distance from the first order Rayleigh line (Rinnan et al., 2005). Here, Rayleigh scatter was removed and Raman scatter was interpolated using the drEEM Toolbox for MATLAB (Murphy et al., 2013) and the methods outlined in Stedmon & Bro (2008).

2.2 Measurement of UV-absorption and spectral slope

Absorbance measurements for all samples were collected on a Shimadzu UV-1800 with a 1 cm cuvette. Six hundred and one absorption spectra were scanned from 200 nm to 800 nm at 1 nm intervals to obtain the absorption characteristics of the samples. Fluorescence measurements were then corrected for instrument specific biases and inner filter effects. Primary inner filter effects occur when incident light is absorbed in a sample before exciting the fluorophore. Secondary inner filter effects occur when light emitted from a flourophore is absorbed before reaching the sensor (Coble et al., 2014). Inner filter correction is implemented into the drEEM Toolbox for MATLAB based on the absorbance method outlined in Lakowicz (2006). To correct for instrument drift, temperature change, and the refractive index, the average absorbance between 700 nm and 800 nm was subtracted from absorbance values (Stedmon et al., 2003). Absorbance units were then converted to Naperian absorption coefficients using equation 1, from Coble et al. (2014):

$$a = 2.303 * A / l \quad (1)$$

Where a = absorption coefficient (m^{-1}), A = absorbance at a specific excitation wavelength, and l = cuvette path length (m). Spectral slope values (S, nm^{-1}) were also calculated for two regions of the collected absorption coefficient spectra, one in a shorter wavelength region (275-295 nm), and one in a longer wavelength region (350-400 nm).

Spectral slopes were calculated according to equation 2, based on methods outlined in Helms et al. (2008).

$$a_\lambda = a_{\lambda ref} e^{-s(\lambda-\lambda ref)} \quad (2)$$

Spectral slope values are mainly independent of CDOM concentration, and can provide more information on the characteristics of CDOM when used in combination with absorption data. Higher slope values derived from equation 2 are indicative of a greater decrease in absorption with increasing wavelength (Helms et al., 2008). Calculating the ratio of the 275-295 nm region and the 350-400 nm region gives a dimensionless value called the slope ratio, given by the variable S_R. Shifts in S_R and $S_{275-295}$ are linked to shifts in molecular weight and photobleaching of CDOM (Helms et al., 2008).

Fluorescence intensity ratio (FIR) values can provide insight into how well oil has dispersed after exposure to chemical dispersant (Bugden et al., 2011). FIR is calculated by dividing the fluorescence intensity at 340 nm emission by the emission at 445 nm (at a constant excitation wavelength of 280 nm). Bugden et al. (2011) defined an FIR value of 4 as the threshold between oils that have been effectively and non-effectively dispersed. Values less than 4 indicate that oil has been sufficiently dispersed (>40%), while values greater than 4 indicate that oil has not been effectively dispersed (<20% dispersion). Fluorescence Intensity Ratio wavelengths can be used to indicate chemical dispersion of oil (Conmy et al., 2014). As such, it provides a dimensionless

value that can be used as an indicator of whether or not oil has been sufficiently dispersed, without having to measure oil concentration (Bugden et al., 2008).

2.3 Measurement of in situ data

Hydrographic data including salinity, temperature, pressure, and oxygen were collected for June and September samples using a Seabird CTD unit mounted onto a steel rosette. Oxygen values are reported in mg/L and are a measure of the dissolved oxygen concentration in a sample. Salinity values are reported in Practical Salinity Units (PSU), which describe the concentration of dissolved salts in seawater. CDOM fluorescence measurements for June samples (in volts) were taken using a WetLabs ECO-CDOM fluorometer (370/460 nm); CDOM measurements for September samples are given in mg/m^3. Chlorophyll-a measurements (µg/L) were taken using a WetLabs fluorometer (470/695 nm), and are an indicator of chlorophyll concentration. DIC values are measured in micromoles/kg, and represent the concentration of DIC per unit mass of seawater. The stable carbon isotope composition ($\delta^{13}C$) of DIC is expressed in per mil (‰) using the delta (δ) convention, and is calculated with equation 3:

$$\delta^{13}C \text{ of DIC} = [(R_{sample} / R_{standard}) - 1] * 1000 \quad (3)$$

Where $R_{sample} = {}^{13}C/{}^{12}C$ in the sample, and $R_{standard} = {}^{13}C/{}^{12}C$ of the Pee Dee Belemnite (PDB) standard (Hansell & Carson, 2014). Samples for $DI^{13}C$ and [DIC] were collected

directly in 2 mL crimp seal vials with butyl rubber septa and stored at 2^{o}C until analysis at the SISIL lab at the Skidaway Institute of Oceanography following Brandes (2009). Potential density anomaly values were calculated using temperature, salinity, and pressure measurements in ODV and are given in kg/m^3. CTD data for the Acadiana Cruise station were also collected using a Seabird CTD unit mounted onto a steel rosette, providing data on temperature (C), salinity (PSU), Oxygen (mg/L), and CDOM (volts). Using CDOM values from the Acadiana Cruise normalized for salinity, the influence of Mississippi River floodwaters was removed by dividing the CDOM signal by 35 and multiplying by the sample salinity, which provided residual CDOM fluorescence values (in volts).

3. RESULTS

3.1 June samples

3.1.1 Proxy in situ data

Hydrographic data provide essential information on the temperature, salinity, and density structure of the water column in the Gulf of Mexico during sampling, and can be used to identify anomalies at depth that may be indicative of oil. For June samples, the surface layer was relatively homogeneous with respect to salinity but showed a consistent temperature increase towards the surface (Figure 3). Temperature values decreased steadily from ~30 °C at the surface to ~4.7 °C below 1000 m. Salinity values were higher from the surface to ~70 m depth, but varied only slightly from the mean of 35.96 PSU for those depths. Salinity then decreased from 70 m to about 600 m depth to a minimum value of 34.90 PSU, and then increased with depth, varying only slightly from the average of 34.94 PSU below 600 m. Density in June samples was driven mostly by temperature, but at stations 4 and 10 higher salinity values at the surface resulted in higher density anomalies until the depth of stratification. The plot of salinity vs. temperature (Figure 3d) reflected the influence of Gulf of Mexico waters in the warmer surface waters for most samples, indicated by higher salinity at temperatures above 20°C. Salinity did not indicate a significant influence of Mississippi river water during the June sampling campaign.

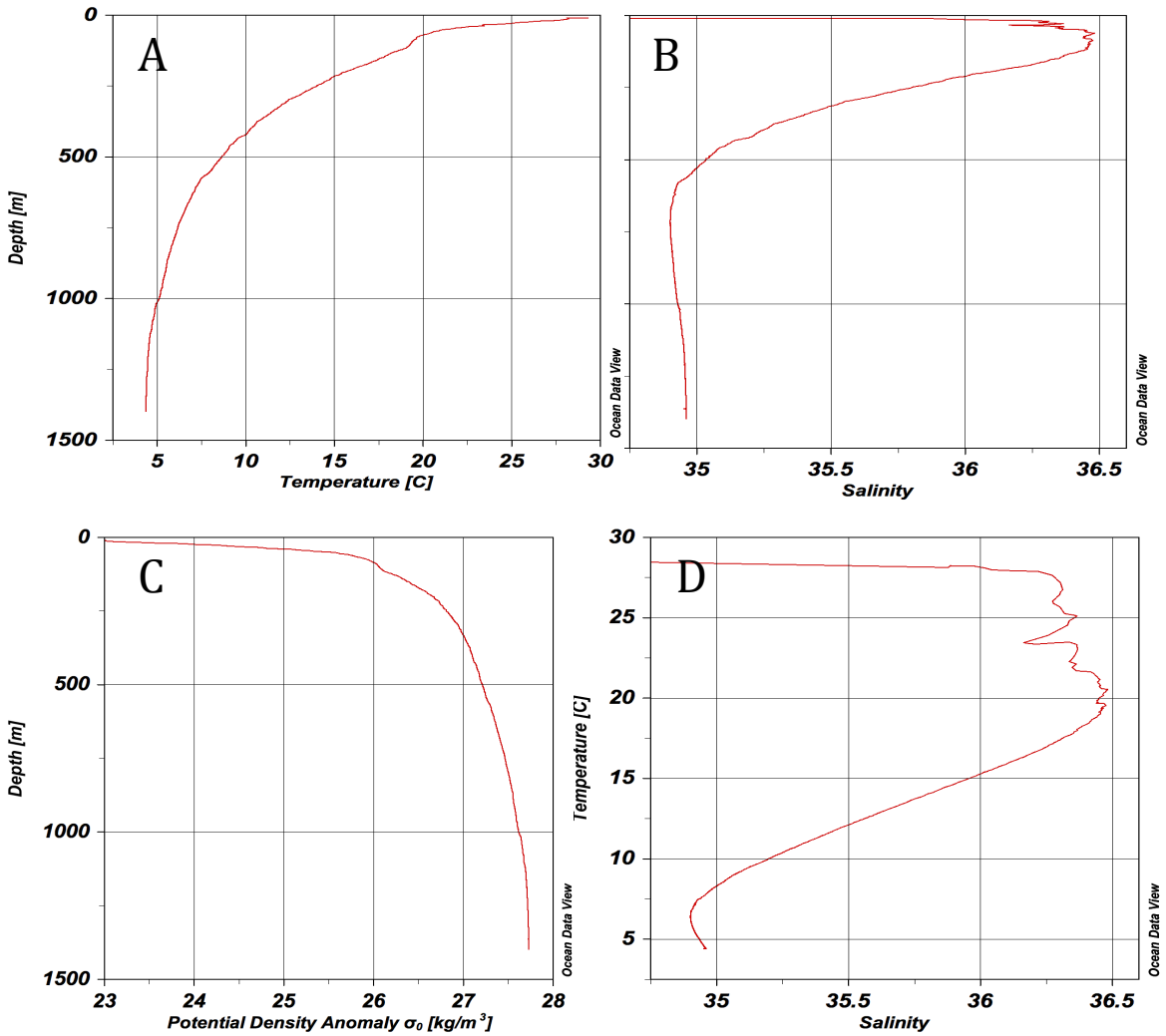

Figure 3: Plot of a) Temperature, b) Salinity, and c) Potential density anomaly vs. depth, and d) Salinity vs. temperature from station 4 (June 2010)

Out of the 60 samples collected during the June cruise, sixteen samples showed characteristics similar to oil, most of them between depths of 1000m and 1300 m. Along with fluorescence signatures from EEMs, these samples showed oxygen depletion, higher CDOM values, spikes in chlorophyll measurements and decreases in transmission (See figure 4 for example).

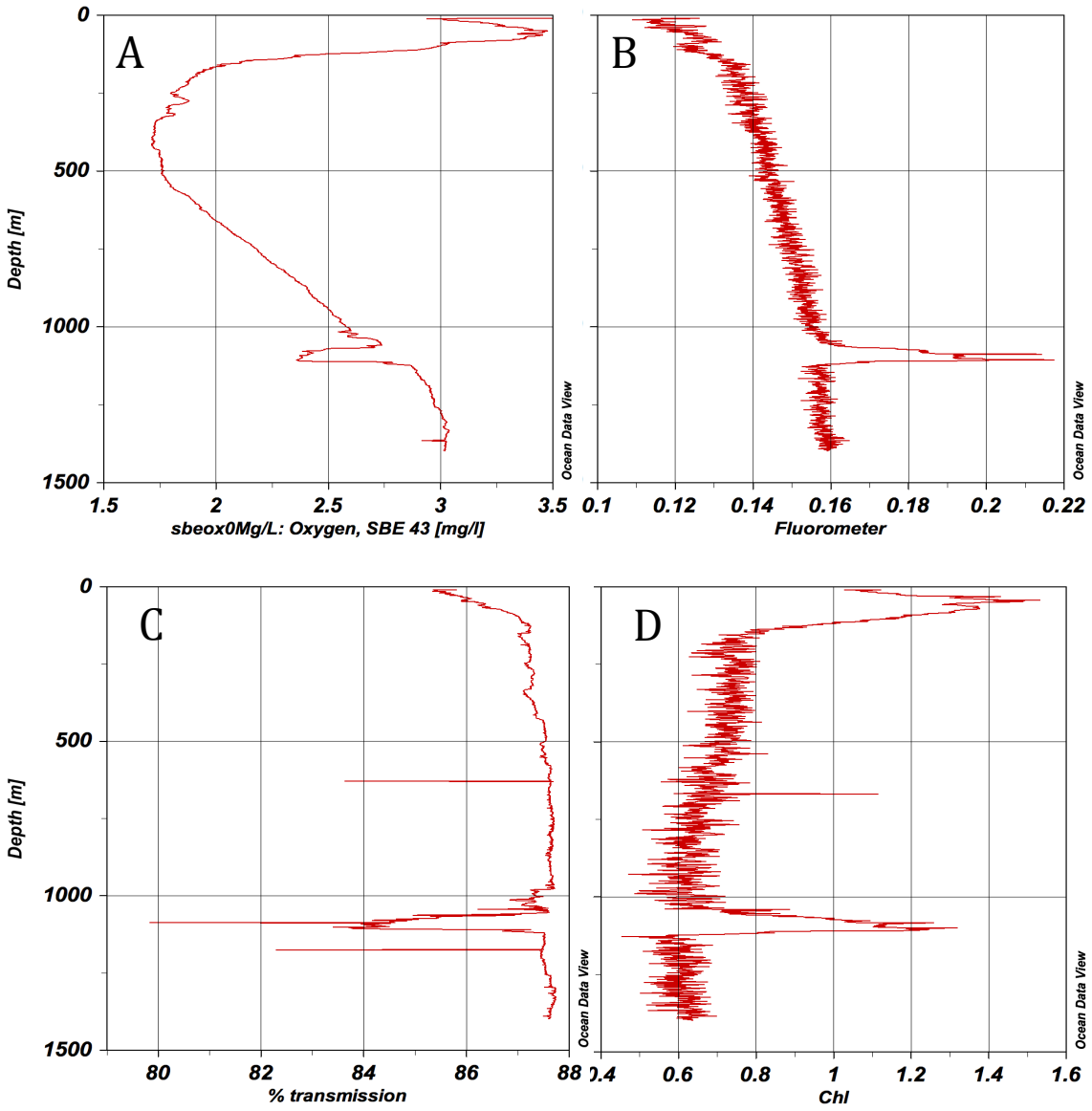

Figure 4: Plot of (a) oxygen, (b) CDOM, (c) transmission, and (d) chlorophyll in situ data from station 4 (June 2010)

Dissolved oxygen values were higher in surface waters, with a mean of 6.02 mg/L down to a depth of 40-60 m, and decreased down to a minimum of ~3.50 mg/L at the oxygen minimum layer around 400 m depth. Values then steadily increased with

depth below 400 m to ~3.1 mg/L at ~1500 m. Much lower oxygen values seen at the surface are the result of lower solubility due to temperature differences. CDOM showed lower values in surface waters (mean 0.12 volts from 0-60 m) and increased steadily with depth to around 0.165 volts at ~ 1300 m, which is primarily due to photobleaching of CDOM in the surface ocean (Nelson & Siegel, 2002). Some stations exhibited increased CDOM around 80 m depth corresponding to the depth of the photic zone. Chlorophyll values were high in surface waters, reaching a maximum of ~1.5 μg/L at 60-70 m depth, corresponding to photosynthesis in the photic zone. Values then decreased steadily with depth to about 0.65 μg/L at 1300 m depth (mean of 0.64 μg/L from 100-1300 m). Transmission values were lower in surface waters to below the photic zone (mean of 85.14 % from 0-100 m), then decreased slightly and leveled off below 100 m depth (mean of 85.53 % from ~100-1300 m).

3.1.2 Spectral slope and slope ratio

Higher $S_{275\text{-}295}$ and S_R values were seen in surface samples as well as those at a depth of around 1100 m (figure 5). $S_{275\text{-}295}$ values from 0-150 m depth had a mean value of 0.03 nm, with the highest values seen at stations 2, 3, 5, 7, 22, and 23. Lower values were seen from 150-1600 m depth; with a mean of 0.021 nm^{-1} seen from 150-1000 m and a mean of 0.022 nm^{-1} from 1000-1600 m. Higher values at ~1100 m depth were found at stations 1, 2, 3, 10, and 25, all located either southwest or northeast of the well. Trends in S_R values were less well defined than those for $S_{275\text{-}295}$. Higher values were

seen at the surface, with a mean of 2.05 from 0-150 m depth. S_R values deeper than 150 m showed variability around the mean of 1.67; however, higher values were seen at ~1100 m depth at stations 9, 10, 15, and 25. Outliers with high values at 460 m and 810 m depth are from stations 22 and 21, respectively, and are both located northeast of the well.

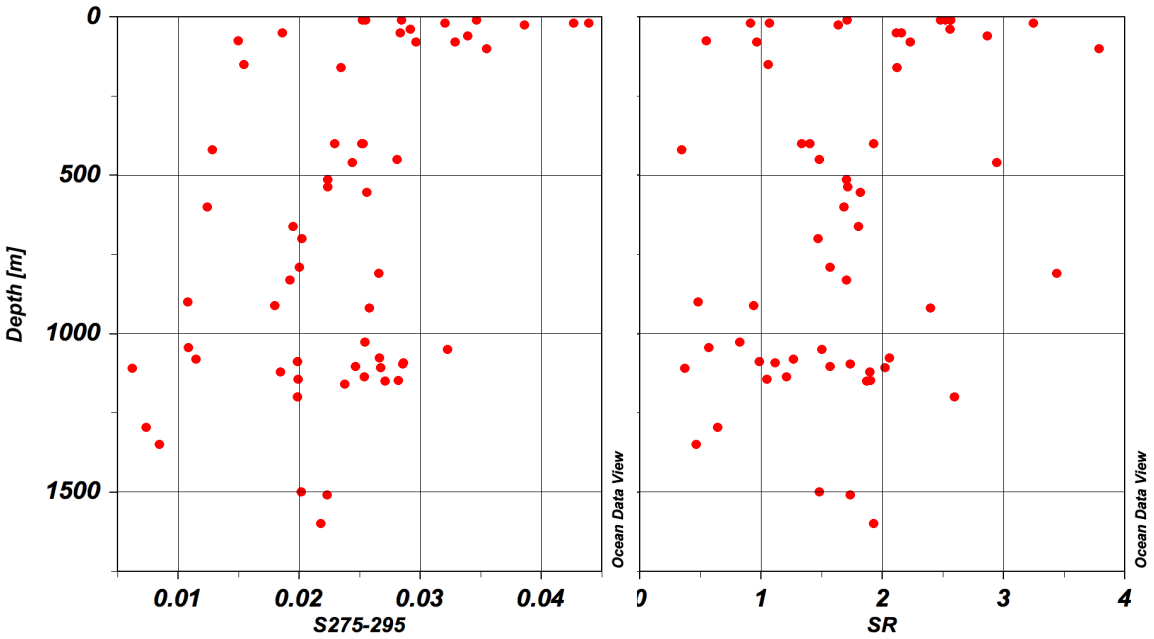

Figure 5: Plot of (a) $S_{275\text{-}295}$ and (b) S_R values for June stations as a function of depth

3.1.3 Fluorescence intensity ratio

The fluorescence intensity ratio values for June stations revealed distinct patterns when plotted as a function of depth (figure 6), with the highest FIR values seen at the surface and also at 1100-1200 m depth. Values from 0-150 m depth had a mean of 4.37

and a maximum of 18.25, with the highest values seen at stations 2, 3, and 5, all located to the southwest of the well. Lower values seen from 150-1000 m depth had a mean of 1.68. Higher values were also seen at depth from 1000-1300 m, with the highest values seen at stations 10, 13, and 25, located to the north and northeast of the well.

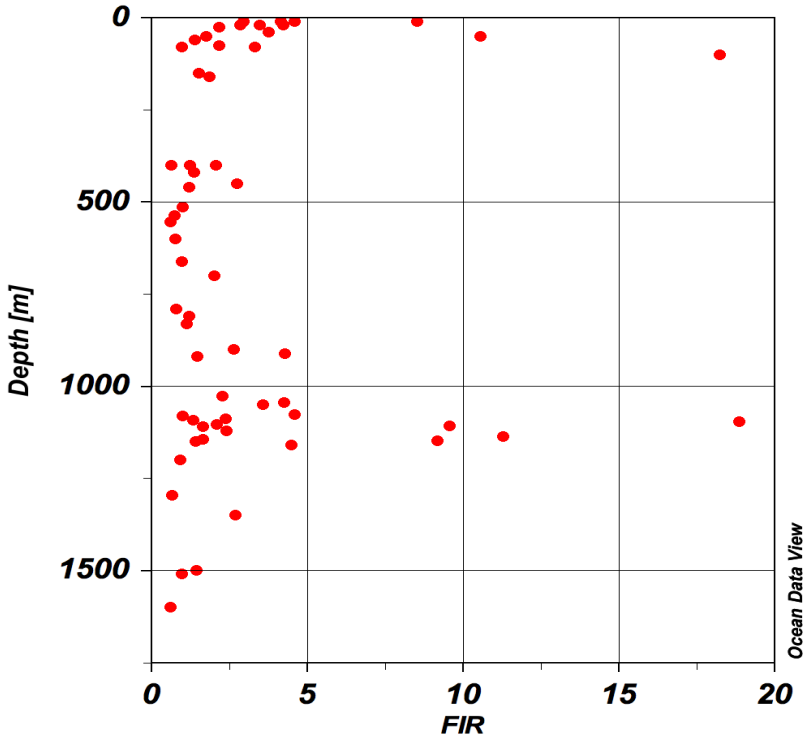

Figure 6: Plot of FIR values for June stations as a function of depth

3.2 September samples

3.2.1 Proxy in situ data

September samples showed stratification around 80 m depth, but the surface layer was not well mixed with respect to temperature and salinity (Figure 7). Similar to June stations, temperature values decreased steadily from ~30 °C at the surface to ~4.7 °C below 1000 m. September stations exhibited lower salinity than June samples, with a mean value of 35.8 PSU in the upper 80 m, which decreased steadily to a minimum of 34.89 PSU at ~625 m. Salinity then increased slightly with depth, with a mean of 34.93 PSU in waters below 625 m. As with June samples, density values were mostly driven by temperature; however, several September samples exhibited density anomalies indicative of a greater influence of fresh water compared to June. The plot of salinity vs. temperature reflected this influence, with lower salinity values that indicated freshwater input in warmer surface waters at stations closest to the well (stations 15-18) (Figure 7d). Stations 1-3 and 8-14 showed similar salinity vs. temperature plots to June samples (seen in figure 3d) indicating source waters from the Gulf of Mexico.

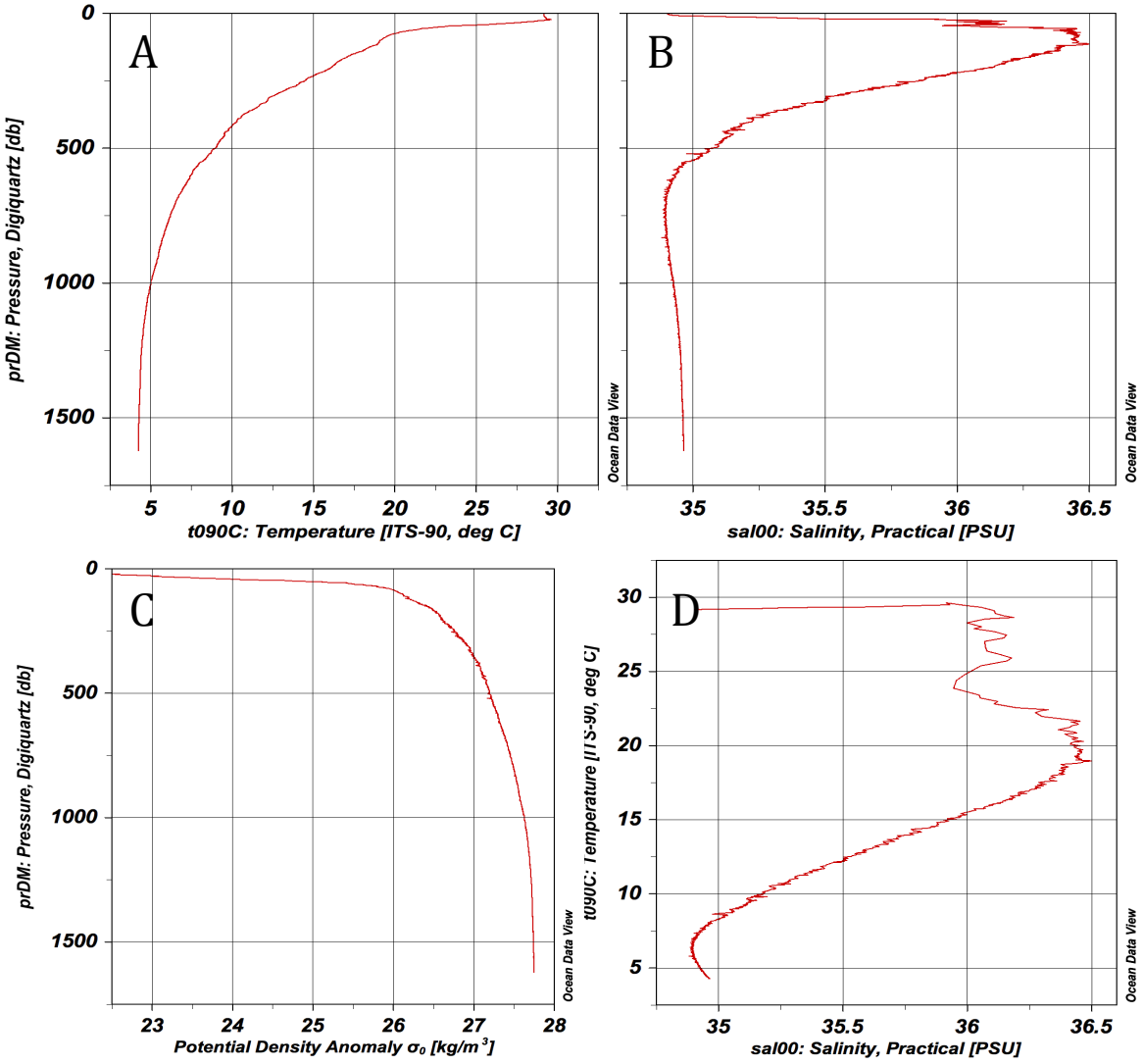

Figure 7: Plot of a) Temperature, b) Salinity, and c) Potential density anomaly vs. depth, and d) Salinity vs. temperature from station 20 (September 2010)

During the September cruise, eight samples showed similar fluorescence signatures to oil between depths of 1000 m and 1200 m, and were concentrated at stations 5, 15, 19, and 20. These signatures were characterized by oxygen depletion, CDOM values higher than baseline, depletion in the $\delta^{13}C$ of DIC, and a spike in DIC concentration (See figure 8 for example).

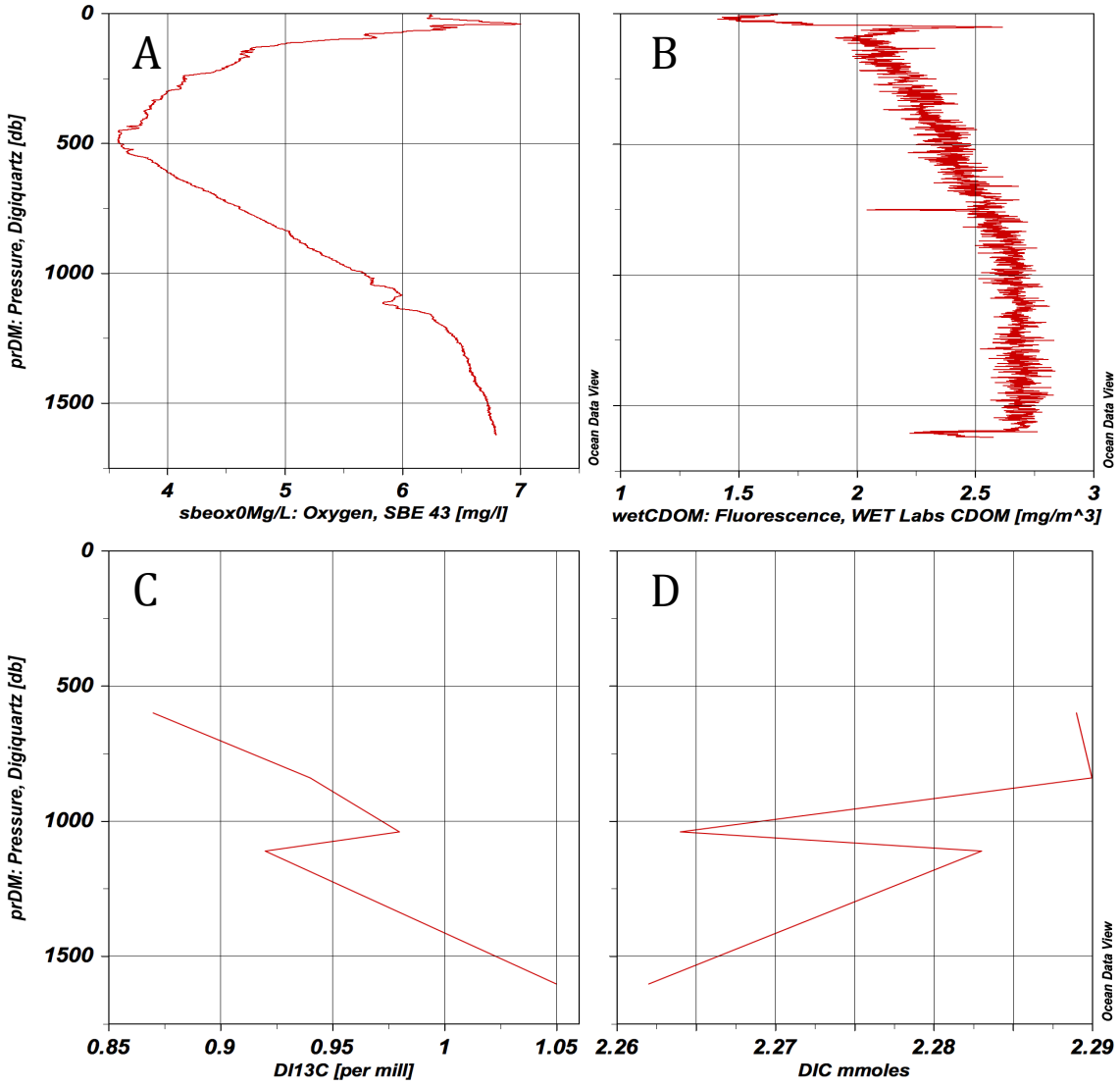

Figure 8: Plot of (a) oxygen, (b) CDOM, (c) $\delta^{13}C$ of DIC, and (d) DIC in situ data from station 20 (September 2010)

Dissolved oxygen values were higher in surface waters, with a mean of 6.32 mg/L down to a depth of 60-70 m. Values then decreased down to a minimum of ~3.65 mg/L at the minimum oxygen layer around 400 m depth, then steadily increased with depth below 400 m to ~6.5-6.8 mg/L. Two stations close to the well (stations 15 and 16) exhibited lower oxygen values (~4.30 mg/L) in surface waters down to ~40 m

depth. CDOM values were lower in surface waters, with a minimum value of ~1.25-1.35 mg/m^3 in the top 50 m of samples. As with June samples, this depletion at the surface was due to photobleaching (Nelson & Siegel, 2002). Values then increased from 60-80 m depth corresponding to the photic zone before decreasing to ~2.00 to 2.10 mg/m^3. Below 80 m, CDOM steadily increased to ~2.70 mg/m^3 at ~900 m depth, then leveled off, slightly varying from the mean value of ~2.66 mg/m^3 below 900 m. Stations 15 and 16, which showed lower oxygen values down to 50 m depth also showed corresponding higher CDOM values. Measurements of DIC and $\delta^{13}C$ of DIC were not collected for every sample, making it difficult to determine trends throughout the water column.

There was a moderate positive correlation between oxygen and $\delta^{13}C$ of DIC ($r = 0.53$, $p = 0.00001$), with depletions in $\delta^{13}C$ of DIC associated with depletions in oxygen (Figure 9). While oxygen and CDOM did not show any relationship ($R^2 = 0.00003$), this is most likely due to insufficient sensitivity in the CDOM sensor; this issue may also be the cause of the positive correlation between CDOM and $\delta^{13}C$ of DIC ($r = 0.37$, $p = 0.00442$). Furthermore, CDOM had a strong negative ($r = 0.71$, $p = 0.00001$) and moderate negative ($r = 0.44$, $p = 0.001$) correlation with $S_{275\text{-}295}$ and FIR, respectively, with higher values for $S_{275\text{-}295}$ and FIR associated with lower CDOM values.

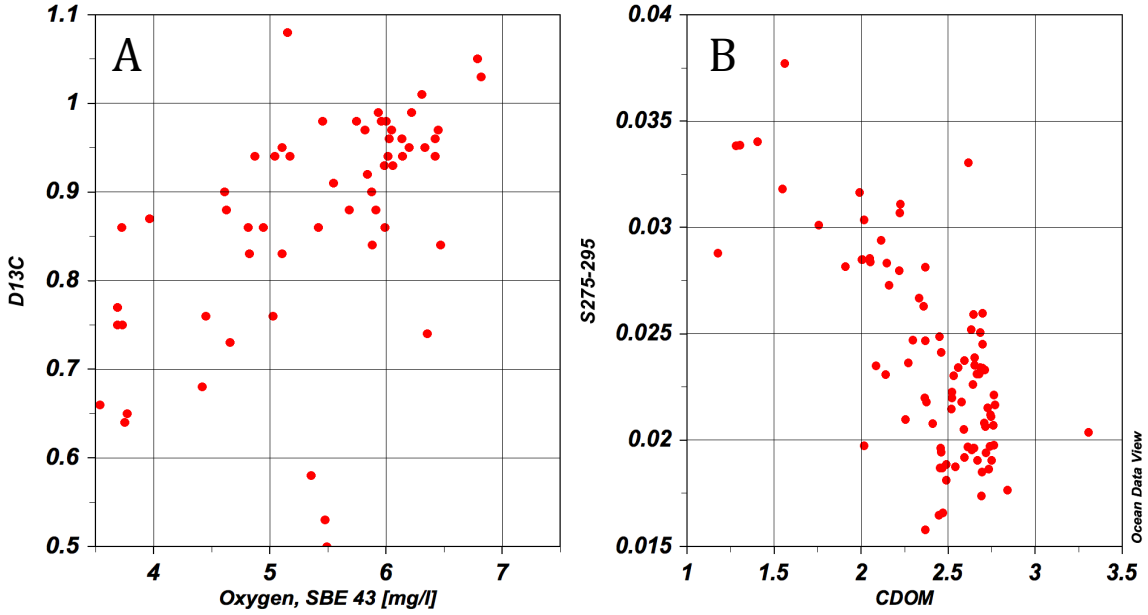

Figure 9: Relationship between a) oxygen values and the $\delta^{13}C$ of DIC and b) CDOM and $S_{275-295}$

3.2.2 Spectral slope and slope ratio

Spectral slope and slope ratio values for September samples showed higher values in surface waters, with mean values of 0.028 nm^{-1} for $S_{275-295}$ and 2.48 for S_R from the surface to 500 m depth (Figure 10). $S_{275-295}$ values decreased below 500 m depth, with a mean value of 0.022 nm^{-1} from 500 m to 1000 m depth, with slightly lower values below 1000 m (mean of 0.0021 nm^{-1}). Slope ratio values followed a similar pattern, with a mean of 1.86 from 500 m to 1000 m depth, decreasing to 1.77 below 1000 m.

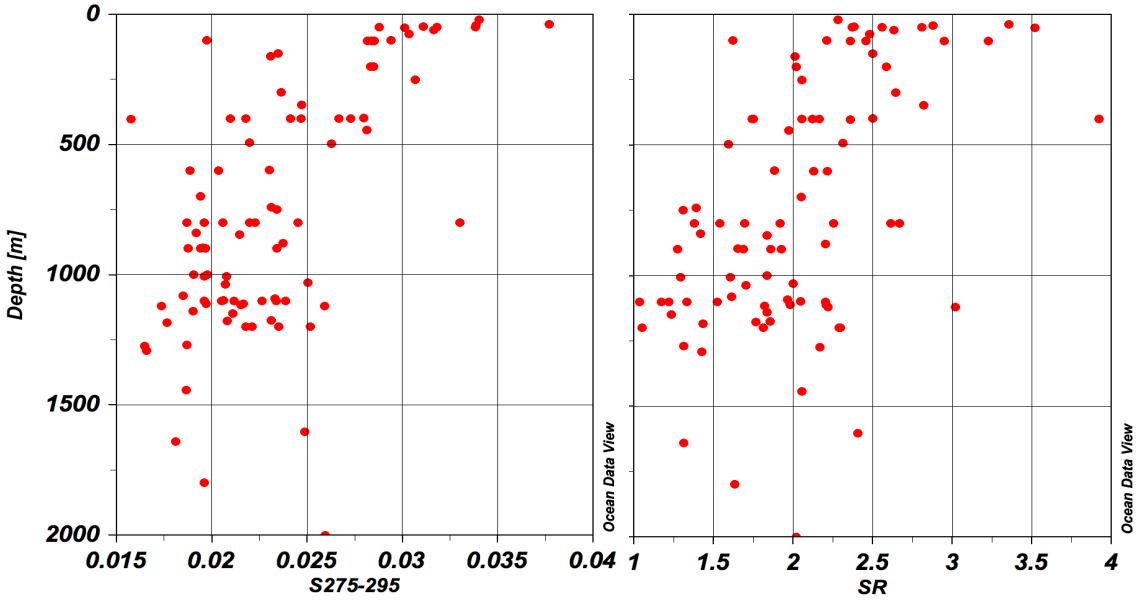

Figure 10: Plot of (a) $S_{275\text{-}295}$ and (b) S_R values for September stations as a function of depth

3.2.3 Fluorescence intensity ratio

When plotted versus depth, FIR values for September stations showed similar trends to June data, with some notable differences (Figure 11). Values were highest from the surface to 400 m depth (mean of 1.57), decreased between 400 m and 800 m (mean of 0.92), and increased from 800 m to 1300 m (mean of 1.24). These values were much lower than those at June stations (mean 1.29 and max 4.55 for September vs. mean 3.30 and max 18.87 for June).

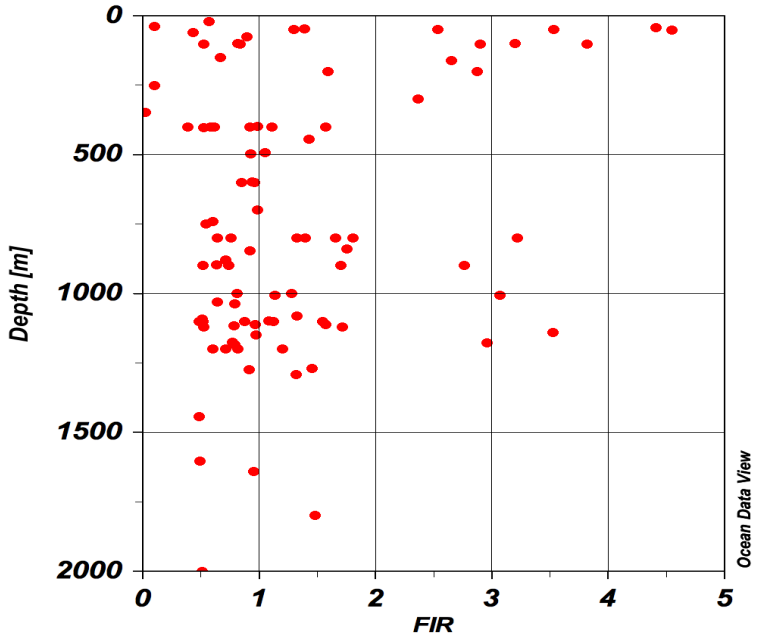

Figure 11: Plot of FIR values for September stations as a function of depth

3.3 Acadiana cruise samples

3.3.1 Proxy in situ data

Hydrographic data from the Acadiana station showed four distinct layers from the surface to 135 m depth (Figure 12). The temperature at the surface was 14°C and increased to 23°C at 11 m. Values were then fairly constant from 11 m to 47 m, decreased to 19.5°C from 48 m to 96 m, and then decreased steadily to ~17.5° at 135 m depth. Similar to temperature, salinity values were lower at the surface, with a minimum of 21.36 PSU, which increased to 35.88 PSU at 11 m. Values then remained fairly

constant, varying only slightly from the mean of 35.91 PSU from 11 m to 135 m depth. Density values clearly indicate the different layers with a ~12m freshwater lens at the surface and three subsequent layers with increasing densities but with variable changes in temperature and salinity. The salinity vs. temperature plot reflected the influence of freshwater at the Acadiana station from Mississippi floodwaters, with low salinity values associated with the lower temperatures seen in surface waters. Inputs of terrestrial organic matter, which are known to have strong fluorescence and absorbance properties, complicated the characterization of samples potentially exhibiting oil signatures.

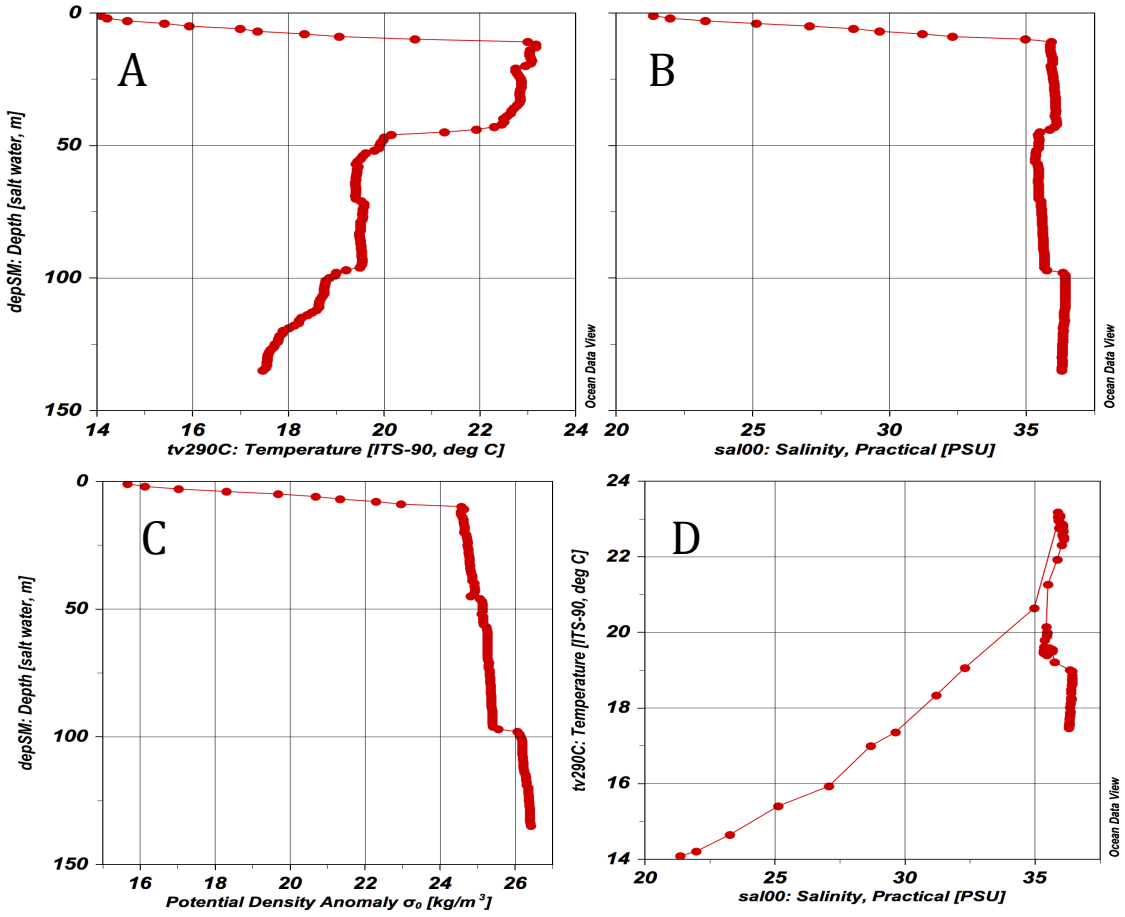

Figure 12: Plot of a) Temperature, b) Salinity, and c) Density vs. depth, and d) Salinity vs. temperature from the Acadiana station

Similar to temperature values, oxygen values for the Acadiana cruise station showed four distinct units from 0 m to 135 m depth (Figure 13). The highest values were seen at the surface, with a value of 8.56 mg/L at 0 m, which then decreased to 5.97 mg/L at 12 m. Values then increased to 6.53 mg/L at 22 m depth before decreasing to 5.72 mg/L at 40m. Between 40 m and 96 m, dissolved oxygen remained fairly constant at ~6.8 mg/L and then decreased, reaching a minimum of ~4.10 mg/L that was constant from 97 m to 135 m depth. This deep layer was potentially sourced from the oxygen minimum layer and advected onto the shelf by coastal upwelling.

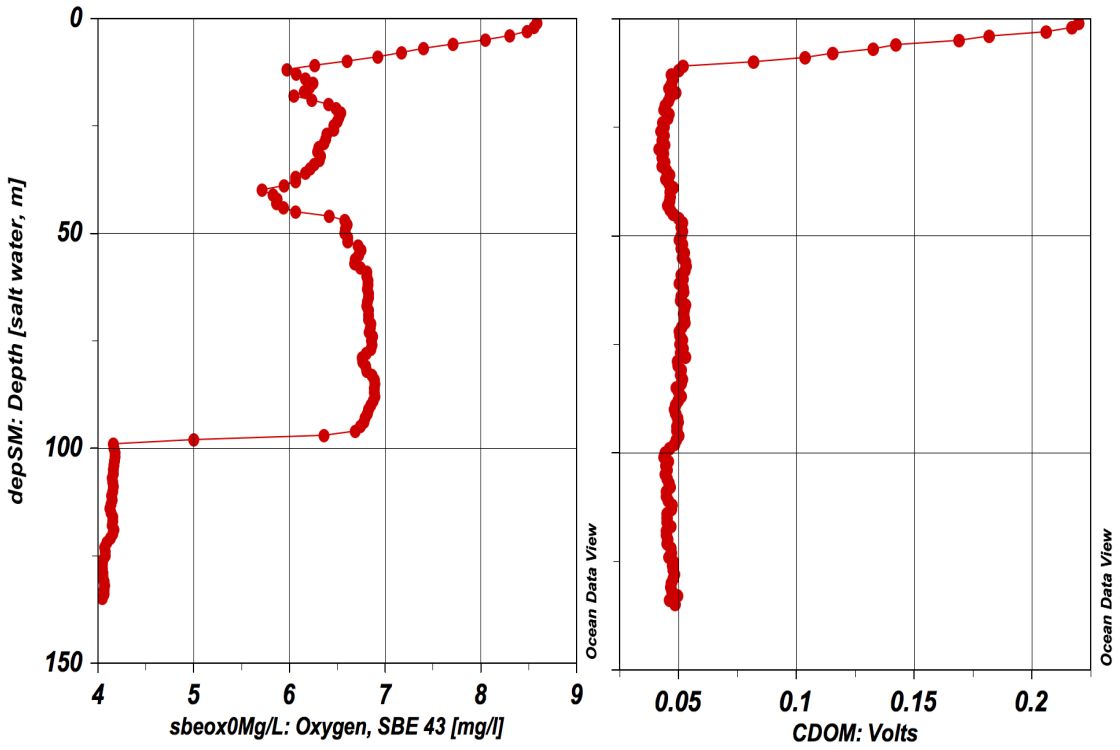

Figure 13: Plot of (a) oxygen, (b) CDOM in situ data from the Acadiana station

CDOM values were much higher at the surface, with a value of 0.22 volts, and then rapidly decreased down to 0.05 volts at 11 m depth. Values from 11 m to 135 m remained constant, varying little from the mean of 0.048 volts. The massive peak seen at the surface, which contrasts with depletions seen at the surface in June and September samples, was due to inputs from Mississippi River floodwaters which reduced salinity on that day to ~21 PSU. After normalizing CDOM values to a salinity of 35 PSU, CDOM values remained elevated down to 11 m depth below which they rapidly decreased to background values. This indicates that once the influence of Mississippi River DOM was removed, 44 % of the remaining CDOM signal was due to some other factor; in this case, a large portion of the residual value was likely due to the presence of oil.

3.3.2 Spectral slope and slope ratio

$S_{275\text{-}295}$ values for the Acadiana cruise station were lowest for the 2 m sample, at 0.016 nm^{-1} (Figure 14). This is in contrast to the June and September cruises, which showed the highest values right at the surface. Values then increased to 0.025 nm^{-1} at 60 m depth, then decreased to 0.018 nm^{-1} for the 112 m sample. The lowest S_R was also seen in the 2 m sample (0.93), which then increased to 2.45 for the 15 m sample, and then decreased to 1.04 for the 112 m sample.

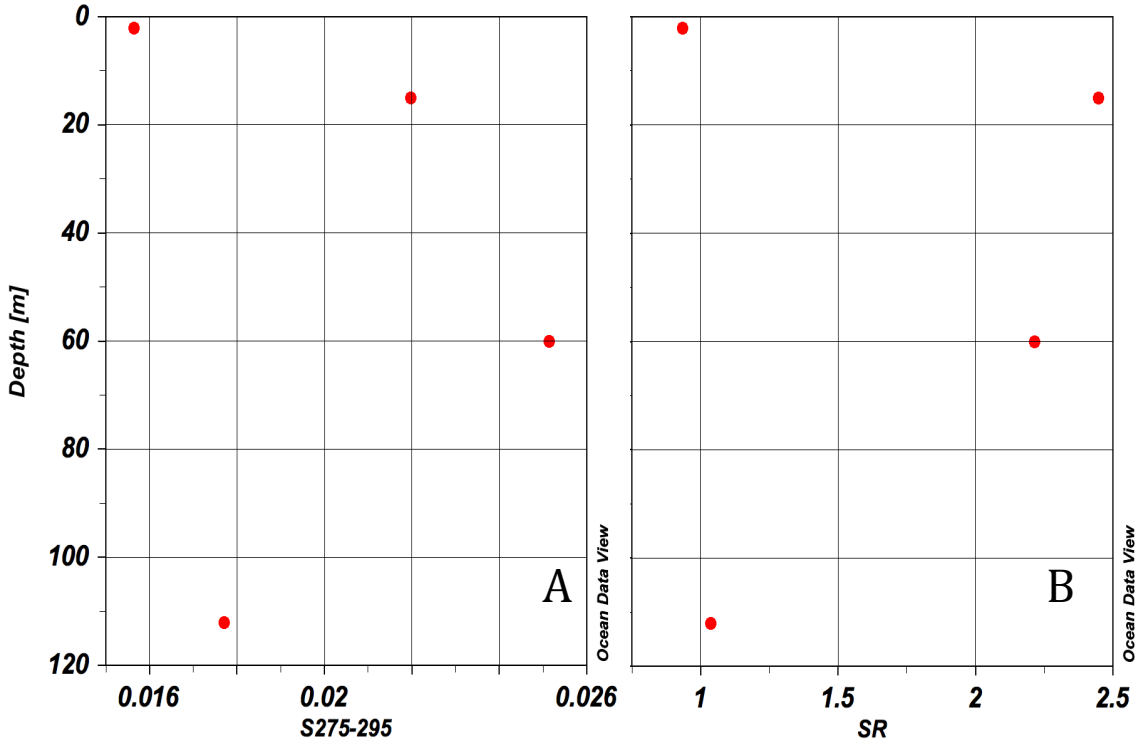

Figure 14: Plot of (a) $S_{275\text{-}295}$ and (b) S_R values for the Acadiana station as a function of depth

3.3.3 Fluorescence intensity ratio

FIR values for the Acadiana cruise station showed a decreasing trend (Figure 15). The highest value was seen for the 2 m sample, with a value of 1.07. Values then decreased steadily to a value of 0.42 for the 112 m sample. These values are not consistent with Bugden et al. (2011), as samples with oil (as was seen at the surface) should have FIR values greater than 4, indicating lower dispersion efficiency. These values are not unreasonable though, considering that the oil was fresh, no chemical

dispersant had been applied, and weathering processes had not had time to significantly affect the oil. Furthermore, visual observations of the oil reported a thin sheen that was more or less constant on the surface, and not a thick layer that would have resulted in higher FIR values.

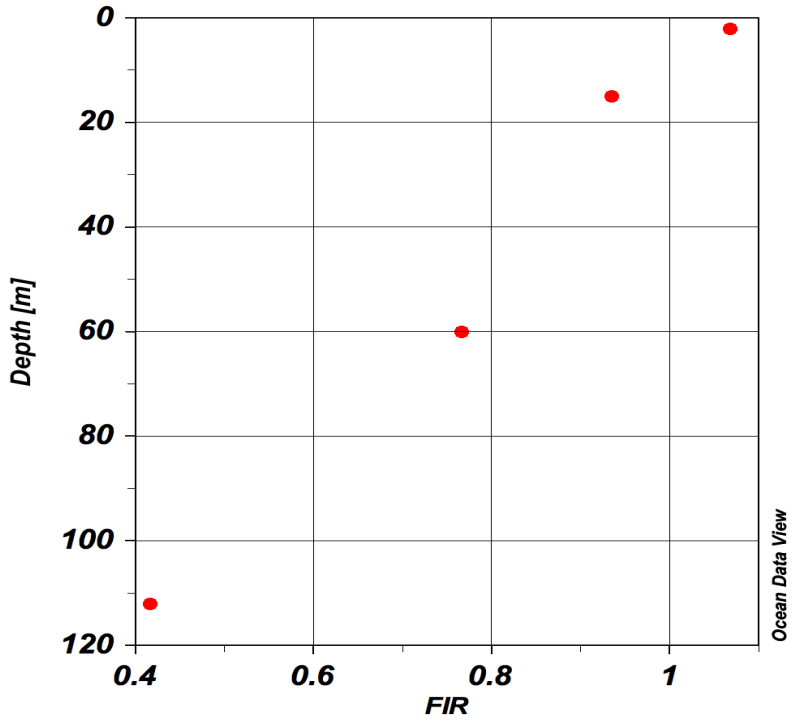

Figure 15: Plot of FIR values for the Acadiana station as a function of depth

4. DISCUSSION

4.1 Excitation/emission wavelength pairs representative of oil

Several sources in the literature reported crude oil peaks below 240 nm excitation (Bianchi et al., 2014; Zhou et al., 2013a; Mendoza et al., 2013; Zhou & Guo, 2012). As the excitation wavelengths run for the June and September stations did not include those below 240 nm, it was not possible to see the full spectrum of these peaks in the fluorescence data; however, signatures of crude oil were evident at excitation wavelengths at or longer than 240 nm. Two pairs of excitation and emission wavelengths were chosen as representative of oil in samples from the Deepwater Horizon spill: 1) 275/324 nm and 2) 240/354 nm. These pairs were chosen based on similarities to crude oil fluorescence signals from the literature, as well as sensor responses seen in measurements of oxygen, CDOM, chlorophyll, and transmission for June samples, and oxygen, CDOM, DIC, and $\delta^{13}C$ of DIC for September samples at depths corresponding to EEMs showing fluorescence characteristics similar to oil.

4.1.1 275/324 nm

The first wavelength pair chosen as representative of oil was centered around 275/324 nm (figure 18c). This signal is similar to the chemically dispersed MC252 signature reported in Conmy et al. (2014). They note that the degradation of light oil that

has been chemically dispersed may increase the presence of longer wavelength peaks, meaning that samples with this signature may be red-shifted from the 270/325 nm peak reported for Macondo crude oil, as in figure 18c. Samples showing the 275/324 nm peak also exhibited higher values around 260/450 nm. Both Conmy et al. (2014) and Zhou et al. (2013a) reported similar signals associated with crude oil mixed with chemical dispersant.

Plotted against depth, the fluorescence intensities for the 275/324 nm pair show higher values in June samples at ~1100 m depth, indicating the presence of dispersants at these depths (Figure 16a). Higher values in surface samples in September may in part be due to a tryptophan-like T peak signal, which can be found at similar excitation and emission wavelengths. Intensity values for the 260/450 nm pair show a distinct difference between the June and September samples, with higher values generally found in September samples at all depths (Figure 16b). Higher values around ~1100 m depth are most likely due to the presence of crude oil mixed with chemical dispersant and the corresponding increase in the humic-like A_C signal, while higher values in surface samples also likely reflect a marine humic-like A_C signal resulting from microbial activity.

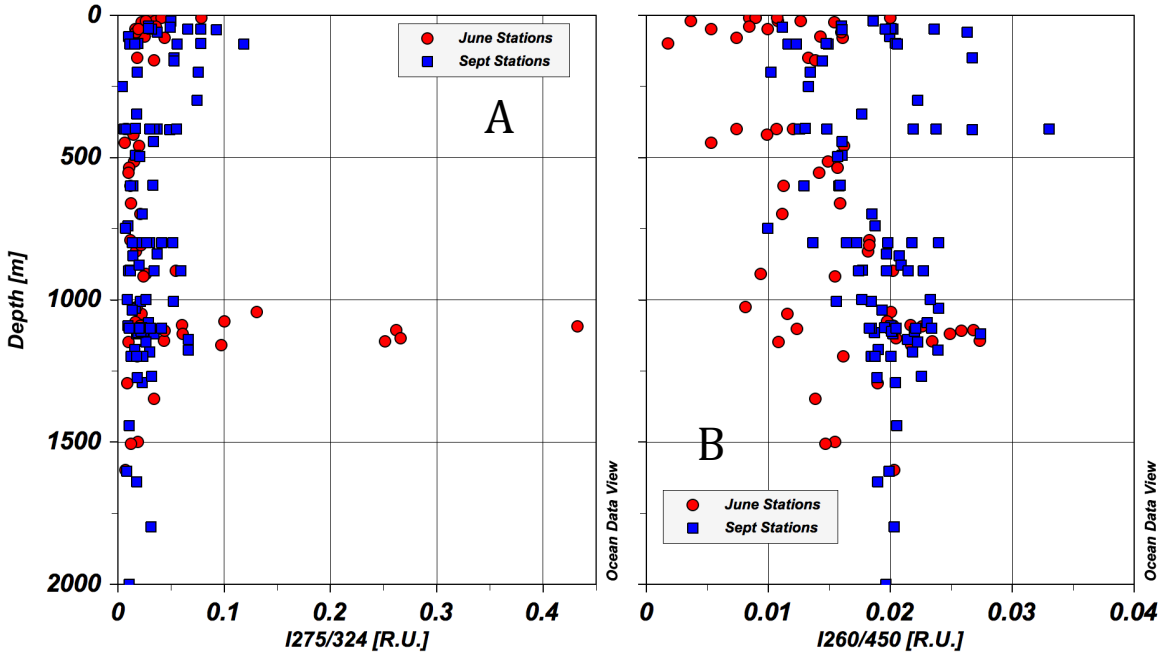

Figure 16: Fluorescence intensity plotted vs. depth for a) 275/324 nm and b) 260/450 nm signals

4.1.2 240/354 nm

The second wavelength pair chosen was centered on 240/354 nm, which shows similarity to both component 3 from Zhou et al. (2013b), identified as a crude oil component, and to component 2 from Zhou et al. (2013a), representing a naphthalene component. Many of the samples exhibiting peaks at 240/354 nm also showed a peak or higher values around 270/308 nm, although in most cases this signature extended from 260-280/300-325 nm (Figure 18d). The location of this secondary peak is similar to that seen in component 6 from Zhou et al. (2013a), which represented a product of crude oil. There was a strong positive correlation between the fluorescence intensity values for the two signals ($R^2 = 0.86$, $p = 0.00001$).

Plotted against depth, the fluorescence intensities for the 240/354 nm and 270/308 nm peaks show trends representative of the presence of oil (Figure 17). The highest values for both wavelength pairs is seen in June samples at a depth of ~1100 m, indicating crude oil at stations near the well during the spill. Lower values at ~1100 m depth in September samples could be a result of the presence of crude oil mixed with dispersants, which causes a red shift in fluorescence intensity values to longer wavelengths (Zhou et al., 2013b; Conmy et al. 2014). The higher values seen in the 270/308 nm signal in September surface samples compared to June may be due to photodegradation; Zhou et al. (2013b) reported a red shift in the secondary peak of crude oil under conditions of photodegration in crude oil samples both with and without dispersant. Fluorescence from a tyrosine-like protein component may also contribute to the higher 270/308 nm signal seen in these surface waters (Coble et al., 2014).

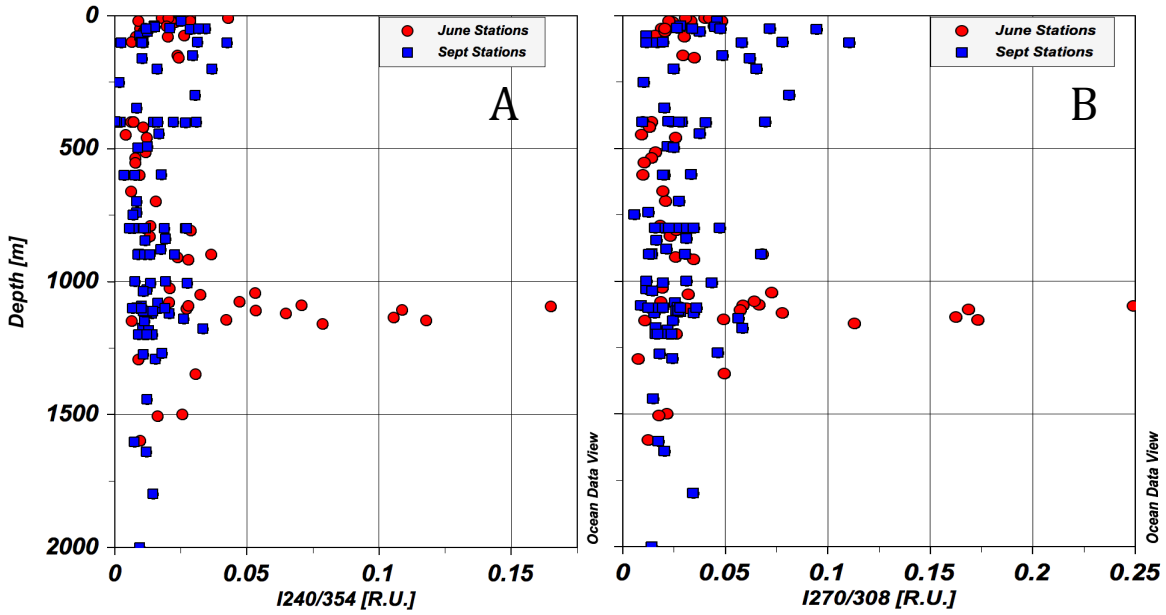

Figure 17: Fluorescence intensity plotted vs. depth for the a) 240/354 nm and b) 270/308 nm signals

4.1.3 Comparison to background signal

Although the EEMs from the June, September, and Acadiana cruises revealed fluorescence signatures indicative of crude oil, comparing these to EEMs exhibiting the background DOM signal in the Gulf of Mexico is necessary to further distinguish between signatures that are specifically representative of oil and those that represent background DOM in a sample. For deep water samples, station 22 at 2000 m depth from the September cruise was chosen to represent the background signal, as it did not exhibit fluorescence optical properties or in situ measurements characteristic of oil. Furthermore, the depth (2000 m) and distance from the well (343 miles) ensured that the sample was representative of open ocean and was most likely outside the influence of oil from the DWH spill. The 2000 m sample showed fluorescence signatures similar to those of C and A_c peaks representative of humic-like DOM of marine origin (Figure 18a) (Coble et al., 2014). At this depth, these peaks are likely due to microbial degradation of oil from hydrocarbon seeps, which are prevalent throughout the Gulf of Mexico (Aharon et al., 1992).

The EEM for station 22 at 50 m depth was used to characterize the DOM signal in shallow waters (Figure 18b). Like the deep water sample used at station 22, this sample was chosen because it did not exhibit optical or in situ characteristics indicative of oil, and because it was located far away from the well (again 343 miles). Similar to the 2000 m sample, the 50 m sample showed C and A_c peaks representative of humic-like DOM of marine origin. These peaks were blue shifted from those seen in deeper waters, which is consistent with microbial and photochemical degradation in marine surface waters (Coble et al., 2014), and is further supported by the M and M_A peaks indicative of biological activity. This could potentially be an oil-derived optical background related to natural hydrocarbon seeps in the area. Also present in the 50 m sample was a tryptophan-like T peak at 275/340 nm.

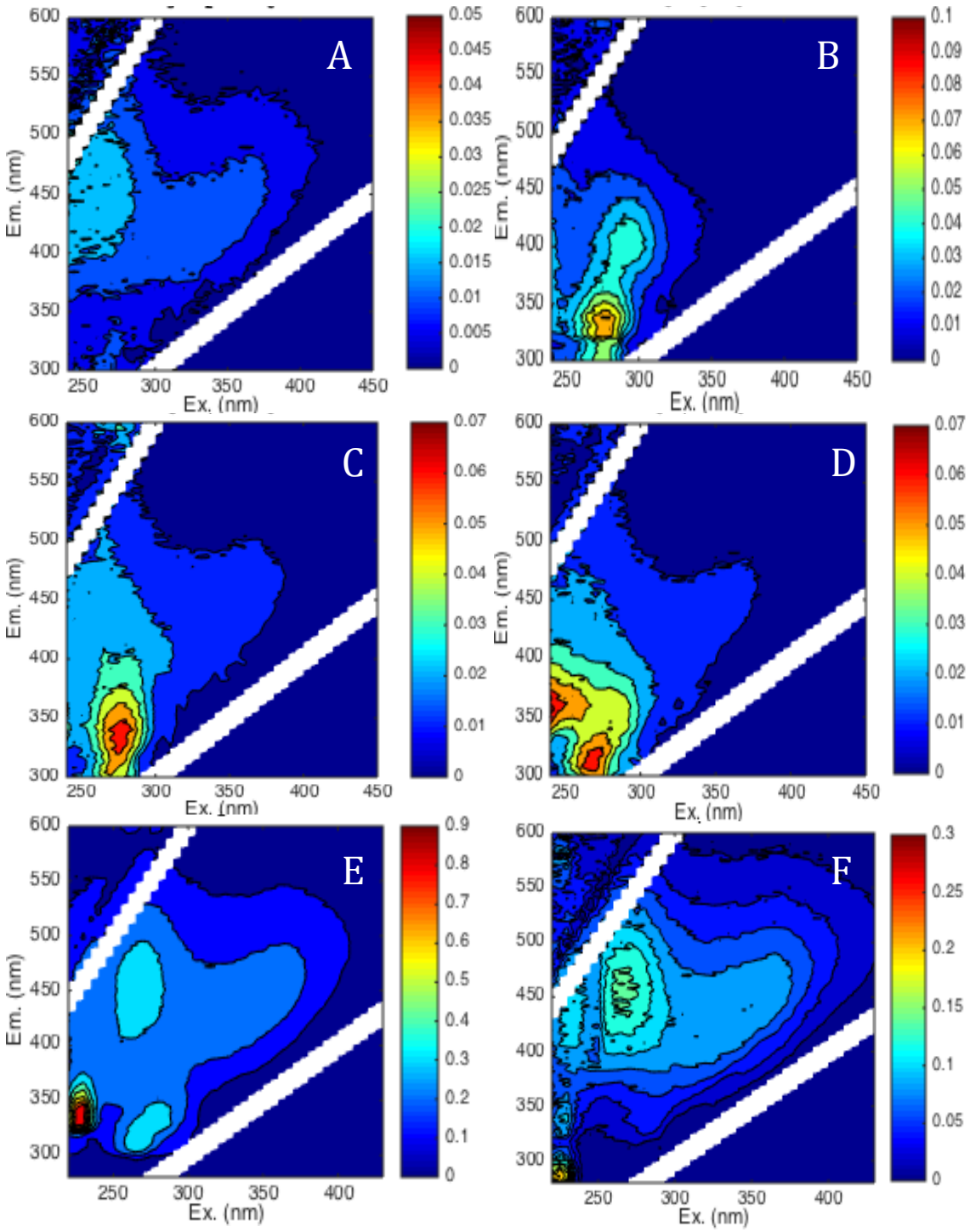

Figure 18: EEMs of a) Background deep water marine dissolved organic matter from station 22 at 2000 m depth (September 2010), b) Background surface marine dissolved organic matter from station 22 at 50 m depth (September 2010), c) The 275/324 nm peak from station 19 at 1078 m depth (September 2010), d) The 240/354 nm peak from station 4 at 1089 m depth (June 2010), e) The sample at 2 m depth (Acadiana), and f) The sample at 112 m depth (Acadiana). Note the different scales for each sample

Most of the June samples and all of the September samples exhibiting the fluorescence characterisitcs of oil also showed the background C and A_c humic-like signatures of marine DOM. Values of C and A_c peak fluorescence intensity values slightly higher in the June and September samples compared to background may be partially explained by the presence of oil; water samples collected near the well exhibited a fluorescence signal associated with oil that extended into the humic-like C peak range (Zhou et al., 2013a). A similar signal was seen in the dichloromethane extract of the DWH oil standard (Guinasso et al., 2012).

4.2 Characterization of June samples

June samples exhibiting characteristic signatures of oil were found between 900 m and 1200 m depth, and generally showed excitation/emission wavelength peaks at 275/324 nm, 240/354 nm, and 270/ 308 nm. These wavelength pairs corresponded to chemically dispersed Macondo crude oil (Conmy et al., 2014) and products of crude oil (Zhou et al., 2013b; Zhou et al., 2013a). Most of the samples that exhibited these peaks also showed higher values in the 260/450 nm region, consistent with increased fluorescence intensity in the 445 nm emission band due to the application of chemical dispersants (Bugden et al., 2008; Zhou et al., 2013b; Conmy et al., 2014). Increased intensity in the 260/450 nm region may also partially reflect the background DOM signal, which showed C and A_C peaks corresponding to marine humic-like organic matter. Hydrographic data showed minimal deviation from background below ~100 m,

indicating that fluorescence signals at depth did not result from differences in temperature or salinity. In situ data for these samples showed depletions in oxygen, increased CDOM fluorescence, increased response of the chlorophyll sensor, and decreased transmission. Coupled with fluorescence EEMs showing peaks similar to oil, these depletions in oxygen and enrichments in CDOM fluorescence indicate that microbial degradation of hydrocarbons occurred at depth in June in the presence of oil.

Absorbance optical properties for June samples provided further evidence of oil at depth. Higher $S_{275\text{-}295}$ and S_R values at the surface and ~1100m depth indicate that degradation from HMW to LMW fractions occurred, possibly due to the presence of chemical dispersants. These higher values in surface waters can partially be explained by photochemical degradation, as irradiation has been shown to increase $S_{275\text{-}295}$ and S_R values (Helms et al., 2008). Higher salinity values in surface waters compared to at depth may also partially explain higher $S_{275\text{-}295}$ down to below the photic zone (Helms et al., 2008). Furthermore, the higher FIRs in surface waters and at ~1100 m depth indicates that oil had not been effectively dispersed at that time (Bugden et al., 2011).

Fluorescence EEMs similar to characteristic oil signatures in the literature coupled with key in situ and absorbance indicators provided evidence of crude oil from the Macondo well at a depth of ~1100 m at stations located between 0-10 miles from the well in June. These optical properties can be compared to those of September stations to

see how the oil spread in the time between the two cruises, and how these properties have changed.

4.3 Characterization of September samples

Samples from September stations exhibiting signatures similar to those of oil were mostly found between 1000 m and 1200 m depth, and showed dissolved oxygen depletion, increased CDOM fluorescence, enrichment of DIC, and depletions in the $\delta^{13}C$ of DIC. Compared to June samples, September samples showed decreased fluorescence intensity in the 275/324 nm and 240/354 nm regions. Decreases in intensity values in the 275/324 nm region are possibly due to signal red-shift from the degradation of crude oil mixed with dispersant. Signals in the 240/354 nm region mostly disappeared in September with the exception of surface samples; this is also likely due to red shift due to a degraded crude oil/dispersant mixture. September samples generally showed increased fluorescence in the 260/450 nm region compared to June samples. While this can partially be explained as the background DOM signal, with C and A_C peaks corresponding to marine humic-like organic matter (Coble et al., 2014), similar increases are consistent with previous studies reporting increases in fluorescence at these wavelengths consistent with the degradation of crude oil mixed with dispersant (Conmy et al., 2014; Zhou et al., 2013a). Several samples that showed this increase also exhibited a signal characteristic of a humic-like A_M peak at 240/350-400 nm and the corresponding humic-like M peak at 290-310/370-420 nm. Hazen et al. (2010) found

depletions in oxygen corresponding to microbial degradation; this partially explains the higher intensity values at emission wavelengths > 400 nm found in September samples compared to June.

As with June samples, the higher values for $S_{275\text{-}295}$, S_R, and FIR at the surface reflect the prevalence of LMW CDOM, and are most likely the result of photodegradation and higher temperatures, as well as greater efficiency of dispersion in surface waters. Higher $S_{275\text{-}295}$ values at 1100 m indicate the dominance of LMW CDOM, which could be due to the dispersion of oil at those depths. However, values at those depths were lower than those found in June samples, which could be the result of microbial biodegradation. Moran et al. (2000) found that microbial degradation caused shifts to lower spectral slope values in samples that had been partially photodegraded. Similar shifts seen at depth in September samples could be the result of microbial degradation in the presence of oil, even in the absence of photodegradation. The much lower FIR values for September stations (mean 1.29 and max 4.55 for September vs. mean 2.88 and max 16.25 for June) indicate that notable dispersion has occurred since the June samples were collected.

September stations generally showed an increase in fluorescence in the longer-wavelength 260/450 nm region. The 275/324 nm, 240/355 nm, and 270/308 nm signatures characteristic of oil were also found, although with generally lower intensities compared to June samples and shifts in the location of peaks. Characterization of

September samples was hindered by incomplete measurements of in situ data. Of the 92 samples collected on the September cruise, 26 samples at stations 8, 9, 12, and 13 did not have any measurements of DIC and the $\delta^{13}C$ of DIC. At other stations, measurements were taken at some depths but not at others, and as such these indicators could not be used at those stations. Ensuring that all samples have corresponding measurements of in situ data would prevent similar issues in the future. Furthermore, collecting measurements of DIC and the $\delta^{13}C$ of DIC for June samples as well as September samples would allow for a more direct comparison between data from the two cruises.

4.4 Characterization of Acadiana cruise samples

Observations of oil on the surface at the Acadiana station provided the opportunity to analyze the optical properties of samples collected from a known oil leak. With the exception of the time required for it to rise to the surface, this oil was fresh and was assumed to be minimally weathered. These samples were then compared to June and September stations for similarities between known oil signatures and those from the DWH spill.

The hydrographic and fluorescence properties of samples from the Acadiana station indicated significant terrestrial influence in surface waters driven principally by inputs from Mississippi River floodwaters shortly before sample collection, with

temperature and salinity values much lower than those seen at June and September stations. Along with the sample taken at 2 m at the Acadiana station, where oil was seen on the surface, the 112 m sample also showed EEM signals representative of oil in the water column (Figure 18e, f). The 2 m sample showed a peak in fluorescence intensity at 225/340 nm, corresponding to crude oil (Bianchi et al., 2014; Zhou et al., 2013a). The 15 m and 112 m sample also showed a peak at 225/340 nm, although the signals at these depths were weaker than in the 2 m sample. Higher values seen around 260-280/305-345 nm likely reflect a combination of tyrosine-like and tryptophan-like protein signatures at the surface. The main fluorescence peak in the 112 m sample was seen at ~225/290 nm and was similar to the weathered oil signature from Bianchi et al. (2014). All four Acadiana samples showed C and A_C humic-like peaks, which can be partially explained by the background marine DOM signal, especially the 112 m sample (Figure 18a); however, additional sources of DOM signal were different depending on the depth of the sample. As the 225/340 nm peak was seen in both the 2m and 112 m samples, part of the DOM signal seen at the surface is derived from oil. This is not surprising given the prevalence of hydrocarbon seeps located on the slope near the station. Coupled with the inputs of DOM from Mississippi River waters, C and A_C DOM signals seen at the surface are possibly a mixture of terrestrial source material and oil that has risen from the seeps.

The absorption properties of Acadiana samples also exhibited terrestrial characteristics. Absorption coefficients for the 2 m sample more closely resembled those

in coastal samples than ocean samples as seen in Helms et al. (2008). The lower $S_{275-295}$ values seen at the surface likely reflect the influence of terrestrial DOM, as decreases in salinity correspond to decreases in $S_{275-295}$ (Helms et al., 2008). This is further supported by the relationship between $S_{275-295}$ and $S_{350-400}$ values; for terrestrial samples, $S_{350-400}$ is greater than $S_{275-295}$ (Helms et al., 2008). Furthermore, much lower $S_{275-295}$ values are seen in the shallow Acadiana samples compared to June and September samples, which reflect the influence of lower salinity waters with DOM of terrestrial origin (Helms et al., 2008). Lower S_R values for the 2 m sample also more closely resemble terrestrial/coastal values (Helms et al., 2008).

The EEMs from the Acadiana station samples did not exhibit the same crude oil signatures as those in June and September. This is partially due to the fact that chemcial dispersant was not applied at the Acadiana station, meaning the 275/324 nm signal would not appear in the Acadiana samples. The different oil peak locations seen in the Acadiana stations did, however, show that although fluorescence optical signals may be noisier below 240 nm excitation wavelengths, oil signatures may be present below these wavelengths which would otherwise be lost when running EEMs above 240 nm Ex.

4.5 Spatial distribution of optical oil indicators

Maps were generated using ODV showing fluorescence intensity values for the 275/324 nm and 240/354 nm wavelength pairs that were chosen as representative of oil

(Figures 19 and 20), and were used to visualize the spread of oil from the DWH spill from June to September at both the surface and at the depth of the oil plume at ~1100 m.

For the June cruise, higher fluorescence intensity values are generally seen both southwest and northeast of the well, with especially high values for both the 275/324 nm and 240/354 nm signals at station 10, located less than two miles from the well. These data are not entirely reflective of the spread of oil in June though, as many stations did not have samples at depths near the surface (represented with a value of 0). Between 900 m and 1200 m depth, the highest intensity values for the 275/324 nm and 240/354 nm signals were seen to the north and northeast of the well. High values can also be seen at station 4 to the southwest, 8 miles from the well. These higher values seen at stations located both northeast and southwest of the Macondo well were consistent with other reports on the spread of the oil after the spill (Mendoza et al., 2013; Zhou et al., 2013a).

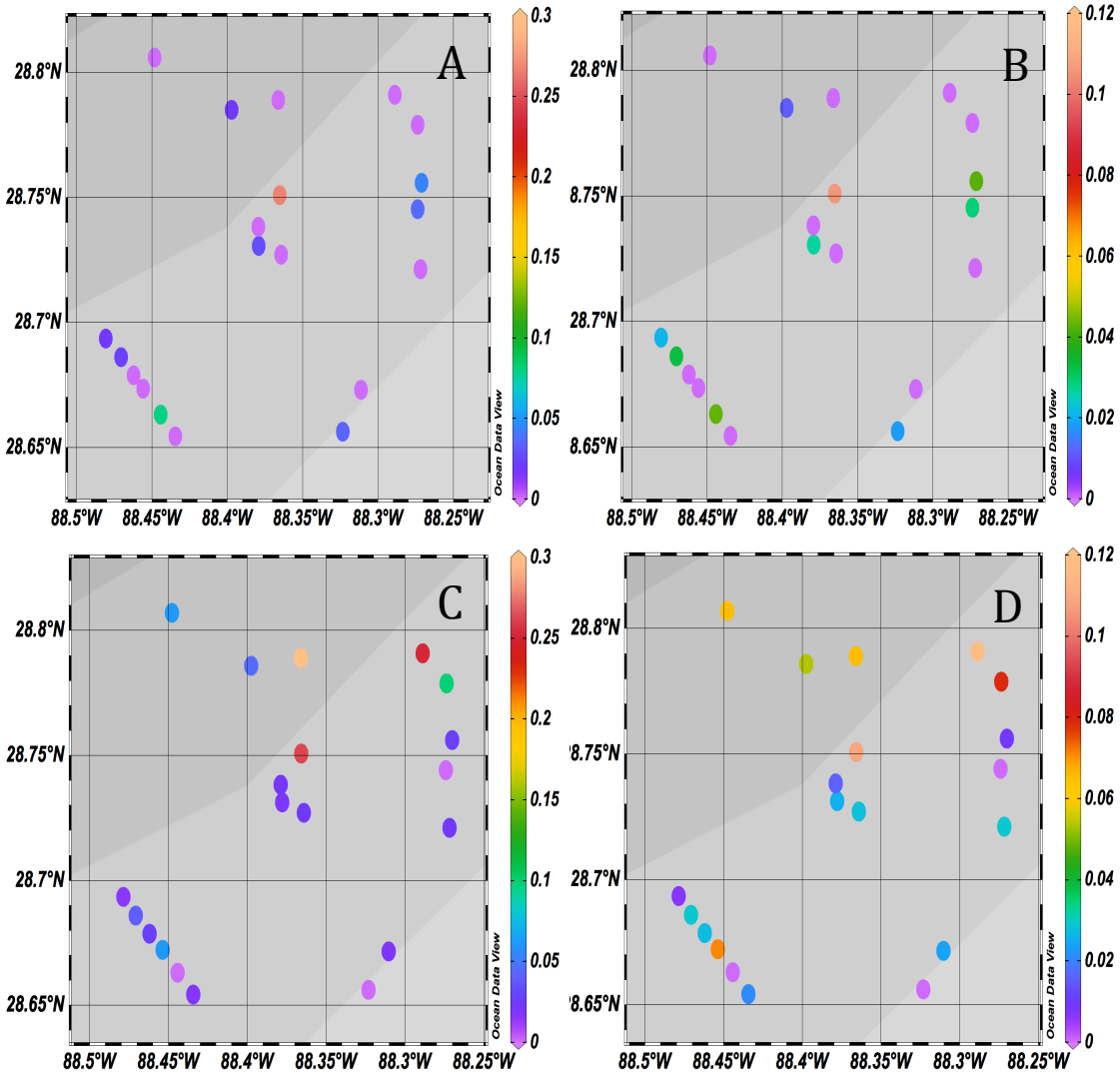

Figure 19: Spatial maps for June samples showing fluorescence intensity values at the surface for a) 275/324 nm and b) 240/354 nm, and between 900m and 1200 m depth for c) 275/324 nm and d) 240/354 nm. A value of 0 indicates that fluorescence data was not collected for that depth interval. Note the different scales for each plot

For the September cruise, surface samples that showed higher fluorescence intensity values at 275/324 nm wavelengths also showed higher values in the 240/354 nm range. These signals appeared in samples up to 280 miles from the well. However,

although the intensity values for the farthest stations (22 and 23) are higher at both the surface and at depth, these samples did not show in situ properties indicative of oil. Again, the surface maps are not entirely reflective of the spread of oil due to a lack of samples at shallow depths. At depth, higher values were seen at stations 8 and 10, both located directly southwest from the well. The farthest sample that showed both a 275/324 nm and a 240/354 nm signal and corresponding proxy indicators of oil was station 5. This indicates that oil from the DWH spill was transported in a subsurface plume almost 300 miles along a southwestward track in the months after the well was capped. Even though oil seeps in the region might also contribute to that signal, the fact that these signals were found at the same density surface as the Macondo oil in June is a strong argument in favor of a Macondo source.

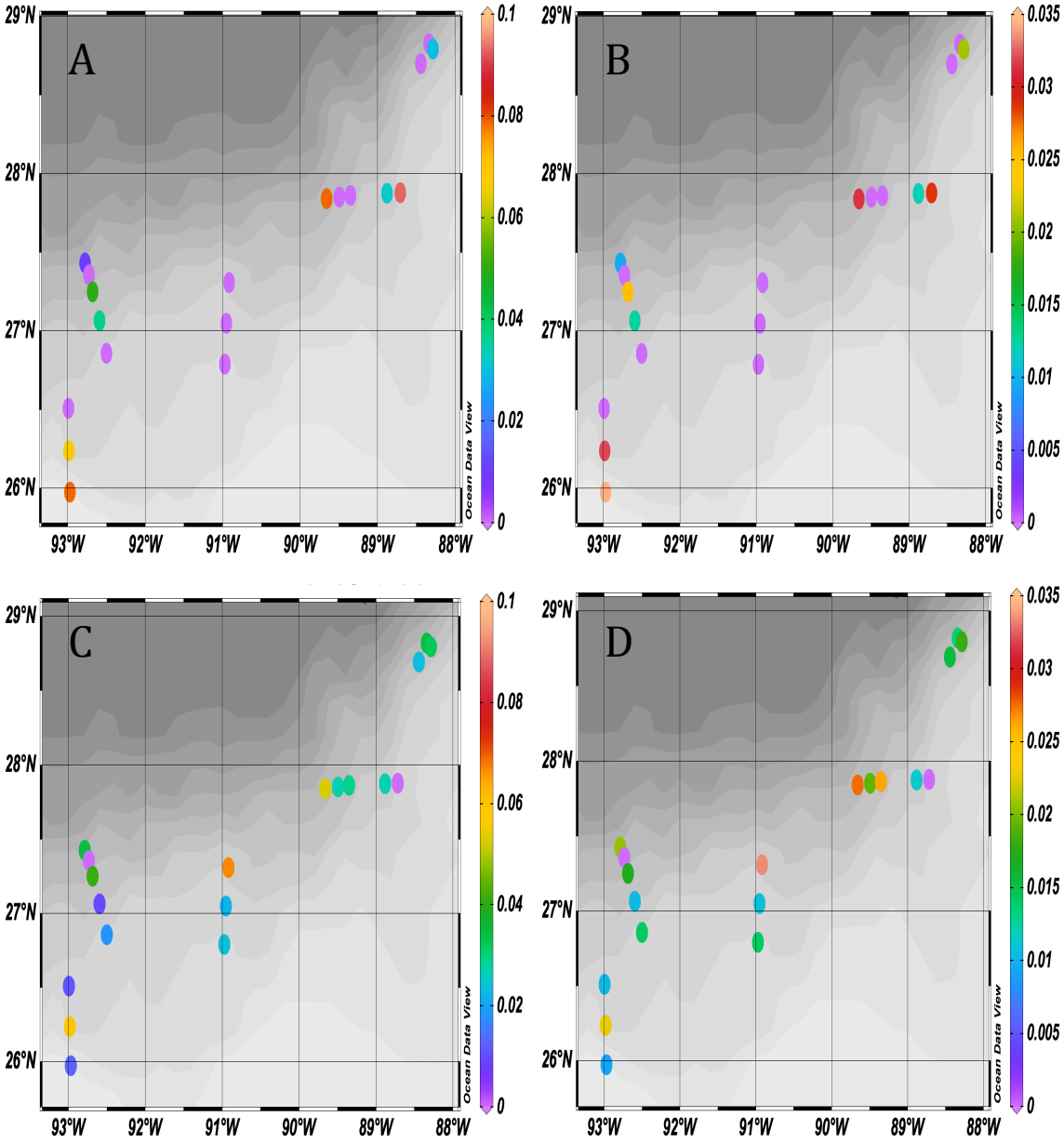

Figure 20: Spatial maps for September samples showing fluorescence intensity values at the surface for a) 275/324 nm and b) 240/354 nm, and between 900m and 1200 depth m for c) 275/324 nm and d) 240/354 nm. A value of 0 indicates that fluorescence data was not collected for the depth interval. Note the different scales for each plot

5. CONCLUSIONS

Water samples were compared from three different cruises in the Gulf of Mexico: One from an area with a fresh oil leak with observations of surface oil, another occurring while the well was still leaking, and a third carried out three months after the well was capped. When coupled with hydrographic information and in situ measurements of proxy data, the fluorescence and absorbance optical properties of oil and seawater samples collected during these cruises aided in understanding the transport and fate of oil from the Deepwater Horizon oil spill. Two excitation/emission wavelength pairs were chosen as indicative of the presence of oil: 275/324 nm and 240/354 nm, corresponding to chemically dispersed oil and crude oil signatures from the literature, respectively. Sensor responses seen in measurements of dissolved oxygen, CDOM fluorescence, DIC, and the $\delta^{13}C$ of DIC were used as in situ indicators for the identification of oil and/or oil degradation. Coupled with fluorescence EEMs, these indicators provided a means to map the spatial distribution of the DWH oil spill in the months after the well was capped. Samples exhibiting oil signatures were generally seen southwest and northeast of the spill in June, before the well was capped. Part of the deep-water plume then travelled along a southwestward track in the months following the spill, with signatures characteristic of oil found at depth almost 300 miles from the well.

There is quite a bit of variability in the literature with respect to EEM scans for characterizing oil components. Further complicating interpretation is the number of different factors that contribute to the fluorescence signal of a sample in addition to potential oil signatures. Special attention must be paid to the characterization of the background signal before quantitative estimates can be made for oil that has potentially been spilled in an area. Furthermore, special consideration must be given to the possible input of terrestrial organic matter from the Mississippi River, which can have significant influence on the fluorescence characteristics of a sample as seen at the Acadiana station. These additional sources are a problem for in situ sensors that cannot "see" wavelengths low enough to effectively characterize oil. Improvements are needed to ensure sensors specifically trace oil without responding to terrestrial DOM or other sources. Finally, it is essential to follow consistent procedures when analyzing the fluorescence optical properties of oil and seawater samples in order to ensure the reproducibility and comparability of results generated by different laboratories.

REFERENCES

Aharon, P., Graber, E. R., & Roberts, H. H. (1992). Dissolved carbon and $\delta^{13}C$ anomalies in the water column caused by hydrocarbon seeps on the northwestern Gulf of Mexico slope. *Geo-Marine Letters*, *12*(1), 33-40.

Bianchi, T. S., Osburn, C., Shields, M. R., Yvon-Lewis, S., Young, J., Guo, L., et al. (2014). Deepwater horizon oil in Gulf of Mexico waters after 2 years: Transformation into the dissolved organic matter pool. *Environmental Science & Technology, 48*(16), 9288-9297. doi:10.1021/es501547b.

Brandes, J. A. (2009). Rapid and precise delta C-13 measurement of dissolved inorganic carbon in natural waters using liquid chromatography coupled to an isotope-ratio mass spectrometer. *Limnology and Oceanography: Methods,* 7: 730-739.

Bugden, J. B. C., Yeung, C. W., Kepkay, P. E., & Lee, K. (2008). Application of ultraviolet fluorometry and excitation–emission matrix spectroscopy (EEMS) to fingerprint oil and chemically dispersed oil in seawater. *Marine Pollution Bulletin, 56*(4), 677-685. doi: http://dx.doi.org/10.1016/j.marpolbul.2007.12.022.

Bugden, J. B. C., Kepkay, P. E., & Johnson, B. D. (2011). The fluorescence intensity ratio (FIR): A new way of assessing the efficiency of oil dispersion. Poster presented at: the International Oil Spill Conference, 23-26 May 2011, Portland, Oregon.

Camilli, R., Reddy, C. M., Yoerger, D. R., Van Mooy, B. A. S., Jakuba, M. V., Kinsey, J. C., et al. (2010). Tracking hydrocarbon plume transport and biodegradation at deepwater horizon. *Science, 330*(6001), 201-204. doi:10.1126/science.1195223.

Coble, P. G. (1996). Characterization of marine and terrestrial DOM in seawater using excitation-emission matrix spectroscopy. *Marine Chemistry, 51*(4), 325-346. doi: http://dx.doi.org/10.1016/0304-4203(95)00062-3.

Coble, P.G., Lead, J., Baker, A., Reynolds, D., & Spencer, R. G. (2014). Aquatic organic matter fluorescence. Cambridge University Press.

Conmy, R. N., Coble, P. G., Farr, J., Wood, A. M., Lee, K., Pegau, W. S., et al. (2014). Submersible optical sensors exposed to chemically dispersed crude oil: Wave tank simulations for improved oil spill monitoring. *Environmental Science & Technology, 48*(3), 1803-1810. doi:10.1021/es404206y.

Diercks, A. R., Highsmith, R. C., Asper, V. L., Joung, D., Zhou, Z., Guo, L., & Wade, T. L. (2010). Characterization of subsurface polycyclic aromatic hydrocarbons at the deepwater horizon site. *Geophysical Research Letters*, *37*(20).

Emerson, S., & Hedges, J. (2008). Chemical oceanography and the marine carbon cycle. Cambridge University Press.

Guinasso, N. L., Wade, T. L., Sweet, S.T., & DiMarco, S.F. (2012). Principle component characterization of fluorescence spectra from seawater samples collected during the deep water horizon oil spill. Poster presented at: the Ocean Sciences Meeting, 20-24 February 2012, Salt Lake City, Utah.

Hansell, D. A., & Carlson, C. A. (Eds.). (2014). Biogeochemistry of marine dissolved organic matter. Academic Press.

Hazen, T. C., Dubinsky, E. A., DeSantis, T. Z., Andersen, G. L., Piceno, Y. M., Singh, N., & Stringfellow, W. T. (2010). Deep-sea oil plume enriches indigenous oil-degrading bacteria. *Science*, *330*(6001), 204-208.

Helms, J. R., Stubbins, A., Ritchie, J. D., Minor, E. C., Kieber, D. J., & Mopper, K. (2008). Absorption spectral slopes and slope ratios as indicators of molecular weight, source, and photobleaching of chromophoric dissolved organic matter. *Limnology and Oceanography*, *53*(3), 955.

Jaffé, R., Cawley, K. M., & Yamashita, Y. (2014). Applications of excitation emission matrix fluorescence with parallel factor analysis (EEM-PARAFAC) in assessing environmental dynamics of natural dissolved organic matter (DOM) in aquatic environments: A review. *Advances in the Physicochemical Characterization of Dissolved Organic Matter: Impact on Natural and Engineered Systems, 1160*, 27-73.

Lakowicz, J.R. (2006). Principles of fluorescence spectroscopy, 3rd ed. New York: Springer Science + Business Media.

Li, Z. (2014). CDOM optical properties near DWH site, gulf of mexico: post oil spill. Doctoral dissertation, Faculty of the Louisiana State University and Agricultural and Mechanical College in partial fulfillment of the requirements for the degree of Master of Science in The Department of Oceanography and Coastal Sciences by Zhi Li BS, Ocean University of China.

Liu, Z., Liu, J., Gardner, W. S., Shank, G. C., & Ostrom, N. E. (2014). The impact of deepwater horizon oil spill on petroleum hydrocarbons in surface waters of the northern gulf of mexico. *Deep Sea Research Part II: Topical Studies in Oceanography,* doi: http://dx.doi.org/10.1016/j.dsr2.2014.01.013.

Mendoza, W. G., Riemer, D. D., & Zika, R. G. (2013). Application of fluorescence and PARAFAC to assess vertical distribution of subsurface hydrocarbons and dispersant during the deepwater horizon oil spill. *Environmental Science-Processes & Impacts, 15*(5), 1017-1030. doi:10.1039/c3em30816b.

Millero, F. J. (2013). Chemical oceanography, third edition. CRC press.

Moran, M. A., Sheldon, W. M., & Zepp, R. G. (2000). Carbon loss and optical property changes during long-term photochemical and biological degradation of estuarine dissolved organic matter. *Limnology and Oceanography*, *45*(6), 1254-1264.

Murphy K.R., Stedmon C.A., Graeber D. and R. Bro (2013). Fluorescence spectroscopy and multi-way techniques. PARAFAC, Anal. Methods, 5, 6557-6566, 2013. DOI:10.1039/c3ay41160e.

Nelson, N. B., & Siegel, D. A. (2002). Chapter 11 - chromophoric DOM in the open ocean. In D. A. H. A. Carlson (Ed.), *Biogeochemistry of marine dissolved organic matter* (pp. 547-VI). San Diego: Academic Press. doi: http://dx.doi.org/10.1016/B978-012323841-2/50013-0.

Schlitzer, R. (2014). Ocean Data View, http://odv.awi.de.

Stedmon, C. A., Markager, S., & Bro, R. (2003). Tracing dissolved organic matter in aquatic environments using a new approach to fluorescence spectroscopy. *Marine Chemistry, 82*(3–4), 239-254. doi: http://dx.doi.org/10.1016/S0304-4203(03)00072-0

Stedmon, C. A., & Bro, R. (2008). Characterizing dissolved organic matter fluorescence with parallel factor analysis: A tutorial. *Limnology and Oceanography: Methods, 6*, 572-579.

Yeh, H. W., & Epstein, S. (1981). Hydrogen and carbon isotopes of petroleum and related organic matter. *Geochimica et Cosmochimica Acta*, *45*(5), 753-762.

Zhou, Z., & Guo, L. (2012). Evolution of the optical properties of seawater influenced by the deepwater horizon oil spill in the gulf of mexico. *Environmental Research Letters, 7*(2), 025301. doi:10.1088/1748-9326/7/2/025301.

Zhou, Z., Guo, L., Shiller, A. M., Lohrenz, S. E., Asper, V. L., & Osburn, C. L. (2013a). Characterization of oil components from the deepwater horizon oil spill in the gulf of mexico using fluorescence EEM and PARAFAC techniques. *Marine Chemistry, 148*, 10-21. doi: http://dx.doi.org/10.1016/j.marchem.2012.10.003.

Zhou, Z., Liu, Z., & Guo, L. (2013b). Chemical evolution of macondo crude oil during laboratory degradation as characterized by fluorescence EEMs and hydrocarbon composition. *Marine Pollution Bulletin, 66*(1–2), 164-175. doi: http://dx.doi.org/10.1016/j.marpolbul.2012.09.028.